BER the international journal of bridge engineering management and research

Modal-Based Multi-Criteria Optimization of Sensor Placement Techniques for Dynamic Monitoring of Bridges

M.G Masciotta[1,2,*]; A. Barontini[3]; E. Chaves[3]; N. Mendes[3]; G. Brando[1,2]; and P.B Lourenço[3]

Submitted: 18 February 2025 **Accepted:** 25 March 2025 **Publication date:** 10 April 2025

DOI: 10.70465/ber.v2i2.26

Abstract: The present work addresses the problem of optimal sensor placement (OSP) for a multi-span concrete bridge, aiming to maximize the informational value of structural health monitoring (SHM) data so that the structural dynamic behavior can be fully characterized with a reduced number of sensors, thereby yielding direct benefits in terms of equipment installation and maintenance costs. To this end, eight distinct optimal sensor placement techniques are examined. Six of these are individual sensor ranking algorithms, whereas the remaining two exploit metrics that evaluate sensor interaction to determine their relevance. Within the first category of algorithms, an enhanced ranking approach based on local maxima is investigated as a promising alternative to improve placement performance and estimate the required number of optimal sensors. The effectiveness of this method is then compared against the second category of algorithms, which are known for their better performance. Extensive experimental data from a well-known benchmark bridge structure are employed to validate this approach, enabling the exploration of a data-driven solution to the OSP problem. By analyzing the advantages and limitations of each algorithm, a modal-based multi-criteria optimization is ultimately applied to drive the selection of the final best sensor configuration for the investigated bridge across multiple scenarios.

Author keywords: Bridge monitoring; optimal sensor placement; heuristics; data-driven OSP; multi-criteria optimization

Introduction

Structural health monitoring (SHM) of bridges is a critical task to ensure the safety and longevity of these vital infrastructures. By continuously tracking and analyzing data on the structural performance of a bridge, SHM systems can detect potential damage, degradation phenomena, or anomalous behaviors early, before they lead to irreversible consequences that threaten the normal infrastructure operation. Recent catastrophic failures, such as the Morandi Bridge in Italy (2018), the Whaley Bridge Dam in the United Kingdom (2019), and the Highway Bridge in China (2024), have highlighted the risks posed by aging infrastructure and the need for more rigorous condition-based maintenance practices. In this context, regular monitoring through sensor network technologies is key to overcoming the limitations of current time-consuming and intermittent inspection routines and to promptly assessing the structural conditions of bridges to make timely informed decisions, thus contributing to a wiser allocation of resources.

Implementing SHM systems for bridges comes with several challenges. Beyond budget constraints, durability issues, and potential difficulties related to the complexity and accessibility of the investigated structures, there are problems associated with the generation of increasingly large volumes of data that can be cumbersome to manage in the long run. Hence, a core aspect of SHM is the strategic placement of sensors, which plays a crucial role in the quantity, quality, and reliability of collected data.[1] This process is known as Optimal Sensor Placement (OSP). In general terms, the OSP problem in SHM seeks to determine the most effective locations where sensors should be installed across a structure to maximize monitoring information while minimizing costs and data redundancy.[2] Indeed, since deploying sensors is expensive, both in terms of hardware and maintenance, and damage can occur in unpredictable locations, not only it is necessary to optimize the number of sensors but also to place them in such a way that they can capture relevant data across a wide range of possible damage scenarios (DSs).[3] Conversely, improper sensor placement can lead to unreliable data and important changes in the structural response may go unnoticed.[4,5]

*Corresponding Author: M.G Masciotta.
Email: G.MASCIOTTA@UNICH.IT
[1]Department of Engineering and Geology, University "G. d'Annunzio" of Chieti-Pescara, 65127, Pescara, Italy
[2]UdA-TechLab, Research Center, University "G. d'Annunzio" of Chieti-Pescara, 66100, Chieti, Italy
[3]University of Minho, ISISE, ARISE, Department of Civil Engineering, Guimarães, Portugal

Discussion period open till six months from the publication date. Please submit separate discussion for each individual paper. This paper is a part of the Vol. 2 of the International Journal of Bridge Engineering, Management and Research (© BER), ISSN 3065-0569.

Various optimization techniques have been proposed in the literature to address the OSP problem, first focusing on aerospace and mechanical applications,[6–9] and then extending the scope to the civil engineering field.[10–16] These techniques aim to find a trade-off between cost, coverage, and sensitivity, ensuring that the SHM system delivers accurate and actionable data for timely maintenance and repairs. Among them, heuristic algorithms represent the most practical approach to finding near-optimal solutions within a reasonable timeframe, though they do not guarantee a global optimum. They are particularly suited when the search space is large and traditional optimization methods involve high computational effort.[17,18] Heuristics place sensors iteratively, assessing step-by-step the contribution of each candidate location to the mode identifiability through the maximization of a specific metric (typically a function of the mode shape matrix). The process continues until a performance threshold is satisfied or a predefined number of sensors providing adequate information for the dynamic identification of the structural behavior is reached. Yet, despite the numerous advantages, heuristics—in their basic version—present inherent limitations that ultimately hinder their successful application: (1) they are often prone to cluster the sensors in a few regions; (2) none of the techniques gives a priori information about the optimal number of sensors to use; (3) the final positioning solutions provided are greatly influenced by the number and characteristics of the selected target modes, namely the most important modes from a dynamic standpoint for the problem at hand; (4) depending on the adopted metric, sub-optimal solutions can vary significantly. On the other hand, a well-established class of heuristic methods achieves optimized placement in a single iteration by ranking sensors according to specific metrics that assess them individually, without considering their interaction and distribution. However, while this approach further enhances computational efficiency, it also increases the likelihood of sensor clustering. Tackling these drawbacks is mandatory to leverage the full potential of heuristics for OSP. In,[10] one of these individual sensor ranking methods was improved by sorting the local maxima of the metric function rather than its maximum values. This strategy, which has received little attention in subsequent literature, not only overcomes the clustering issue but also provides a rapid approach to determining the optimal number of sensors required for a given set of target modes.

Rooted in the research framework outlined above, the present work explores eight distinct OSP techniques for the health monitoring of multi-span bridges. Six of them are individual sensor ranking algorithms, whereas the other two rely on metrics that assess sensor interaction to determine their relevance. By analyzing the former class of algorithms, a promising alternative ranking solution based on local maxima is explored to enhance the final placement performance and provide an estimate of the required number of sensors. This solution is then compared with the second class of algorithms, known for their superior performance. Existing studies in the literature typically focus on a limited number of methods, often restricting their analysis to a straightforward comparison of performance metrics. Instead, the present study moves forward by conducting an in-depth assessment of the advantages and limitations of each algorithm and proposing a modal-based multi-criteria optimization. This approach allows identifying the best possible sensor configuration—among all potential sub-optimal candidates derived from the analyzed techniques—which ensures the retention of the most important modal information about the system under investigation, even in the presence of changing structural conditions. Data from a real well-known bridge structure are employed to validate this novel approach, enabling the exploration of an emerging data-driven solution to the OSP problem. This solution aims to overcome the limitations of the traditional model-based approach. Although more experimentally intensive, it avoids the typical uncertainties and potential sources of error inherent to generating a reliable numerical model of the structure. Instead, it directly assesses the actual response of the bridge under operating conditions. The selected experimental benchmark consists of 108-channel datasets acquired under varying structural scenarios via multiple setups through a dense sensor network deployed on top of the bridge deck. To the best of the authors' knowledge, there are no works in the literature addressing the OSP problem for bridge monitoring with such an extensive and granular set of DOFs measured under changing structural configurations. Indeed, the higher the spatial density of the SHM system, the greater the monitoring fidelity, and hence the more accurate the evaluation of the algorithms' performance when minimizing the number of sensors. The reminder of the paper is organized as follows. Section 2 provides a concise overview of the most recurrent OSP techniques employed for bridge monitoring. Section 3 presents a detailed analysis of the performance metrics of the investigated algorithms, resorting to analytical examples of beam-like systems under different boundary conditions. Section 4 investigates the goodness of the analysed OSP algorithms through a modal-based multi-criteria optimization approach with application to a real-world case study and explores alternative ranking solutions to guide the selection of the final best sensor placement among different candidate configurations. Finally, Section 5 summarizes the main conclusions drawn from this study.

State-of-the-Art OSP Techniques

The OSP task for vibration monitoring can be mathematically expressed as a combinatorial discrete constrained black-box optimization problem. It involves the definition of s optimal sensor locations and d acquisition directions for any location, out of a set of n feasible candidates, to identify m target modes.[19] Being the set of candidate solutions finite and pre-determined, it can theoretically be solved by brute force, testing all the possible combinations in the search space. However, this is not practically feasible in real-life cases due to limited computational capability. By contrast, heuristic procedures can be employed to explore the search space partially, thus drastically reducing the computational burden, and to find a near-optimal solution that should be sufficiently close to the actual optimum.[3] In this section,

the most recurrent heuristic algorithms available in the literature and suitable for data-driven OSP in the context of bridge monitoring are presented by briefly recalling their basic formulations and working principles. Specifically, eight heuristic algorithms are investigated: (i) non-optimal driving point (NODP); (ii) eigenvalue vector product (EVP); (iii) mode shape summation plot (MSSP); (iv) average drive point residue (ADPR); (v) weighted average drive point residue (WDPR); (vi) variance method (VM); (vii) QR decomposition (QRD); and (viii) effective independence (EfI).

The NODP algorithm aims to avoid placing sensors in near-nodal areas of the mode shapes, where signals may be weak or noisy.[20] To achieve this, the algorithm selects sensor locations based on the largest minimum mode shape displacement across the target modes, maximizing the following metric:

$$\mathrm{NODP}_i = \min_j \left|\Phi_{ij}\right| \tag{1}$$

While this method prevents the selection of points where motion is minimal, it does not guarantee the selection of high-response locations. In contrast, the EVP and the MSSP algorithms[21,22] aim to place sensors at locations where the target mode shapes exhibit the largest contributions by maximizing the following metrics, respectively,

$$\mathrm{EVP}_i = \prod_{j=1}^{m} \left|\Phi_{ij}\right| \tag{2}$$

$$\mathrm{MSSP}_i = \sum_{j=1}^{m} \left|\Phi_{ij}\right| \tag{3}$$

Through this approach, the methods analyse the combined effect of multiple mode shapes by selecting measurement points that ensure significant displacements across more modes. At the same time, they reduce the likelihood of selecting near-nodal areas for certain modes, as these locations would not contribute to increasing the MSSP and could even reduce the EVP to nearly zero. The maximization of the modal displacements across the target modes is also pursued by the ADPR and the WDPR methods.[23] Both methods rely on the estimation of the driving point residue (DPR) matrix, as follows:

$$\mathrm{DPR} = \Phi \otimes \Phi \Lambda^{-1} \tag{4}$$

where $\mathbf{\Lambda}$ is the diagonal matrix of angular frequencies and $\otimes$ is the term-by-term matrix multiplier. The ADPR method maximizes the average DPR across multiple modes:

$$\mathrm{ADPR}_i = \frac{1}{m} \sum_{j=1}^{m} \mathrm{DPR}_{ij} \tag{5}$$

Since this approach may overlook localized low responses for specific target modes, the WDPR maximizes the former, weighted by the minimum absolute value of the DPR across the rows. This prevents the selection of nodes in low response regions.

The VM aims to select measurement points that ensure strong signal strength and high-quality reconstruction of mode shapes at unmeasured locations.[10] This is achieved by maximizing the ratio between the diagonal terms c_{ii} of the covariance matrix of the transpose of the mode shape matrix and the sum of the corresponding off-diagonal terms.

$$\mathrm{VM}_i = \frac{c_{ii}}{\sum_{j=1, j\neq i}^{n} c_{ij}} \tag{6}$$

While the off-diagonal terms attempt to account for sensor interactions that were overlooked by previous methods, the VM still suffers from sensor clustering, similar to previous algorithms.

The last two methods, namely the QRD and the EfI, fully account for the interaction of the sensors. The QRD method[24] applies the well-known QRD to the mode shape matrix as follows:

$$\Phi^{\mathrm{T}} P = QR \tag{7}$$

where Q is an orthogonal matrix, R is an upper triangular matrix with decreasing diagonal elements, and P is a permutation matrix whose first m columns identify the best locations ranked by the method. This makes it a single-iteration method as well. The selected locations provide linearly independent mode shapes; however, a limitation of the method is that the number of best locations must be equal to the number of target modes.

Finally, the EfI method[25] aims to ensure high mode identifiability by maximizing the determinant of the Fisher information matrix (FIM). At each iteration, the FIM is computed by partitioning the target modal matrix to the s retained sensor locations:

$$\mathrm{FIM} = \Phi_{sm}^{T} \Phi_{sm} \tag{8}$$

Then, the method rejects the location with the lowest value in the effective independence distribution:

$$\mathrm{E}_d = ([\Phi_{sm}\Psi \otimes \Phi_{sm}\Psi]\lambda^{-1})1 \tag{9}$$

where Ψ and λ are the eigenvectors and eigenvalues of the FIM, respectively, and 1 is the unitary column vector.

Analysis of Current OSP Algorithms through Analytical Data

To thoroughly investigate the effectiveness of the aforementioned heuristics and highlight the drawbacks that most hinder the wide applicability of current OSP techniques, applications to four analytical examples are showcased. These examples concern a single-span concrete beam with a hollow cross-section subjected to different boundary conditions, as illustrated in Fig. 1: (1) simply supported concrete beam; (2) clamped-supported concrete beam; (3) clamped-clamped concrete beam; and (4) cantilever concrete beam. In each case, the beam features a length of 30 m, a cross-section with a 6 m base, 1 m height, and 0.35 m thickness, a Young's modulus of 30 GPa, and a density of 2500 kg/m^3. The primary goal of this analysis is to assess the performance of single-iteration individual sensor ranking methods (EVP, MSSP, ADPR, WDPR, NODP, and VM) in comparison to heuristics that account for sensor interaction (EfI and

QRD). The aim is to identify their limitations and propose potential solutions, focusing particularly on mitigating clustering in the final sensor locations and determining the optimal number of sensors. To ensure consistency across all boundary conditions, the number of potential sensor locations is set to 100 candidates evenly distributed along the beam length, while the number of target modes varies from a minimum of three to a maximum of seven modes. For simplicity, the analyses are confined to bending modes in the vertical plane (Fig. 2), and only uniaxial sensors are considered.

Figs. 3 to 8 show, for each instance, the spatial variation of the metrics considered by the individual sensor ranking methods and the optimized locations computed using a standard approach, in which the final number of sensors is set equal to the number of target modes. It is observed that, except for the NODP and WDPR algorithms, most heuristics tend to cluster sensors within specific regions of the beam. This well-known limitation is likely exacerbated by the large number of considered candidates and could be mitigated by an initial filtering of possible locations. For more complex structures, this may require a high level of knowledge of their dynamic behavior. Clustering can lead to uneven monitoring coverage and reduced effectiveness of the sensor network. In contrast, a well-distributed sensor network increases the likelihood of detecting localized anomalies compared to a clustered arrangement.

To solve the problem of sensor clustering and enhance spatial coverage, the local maxima of the metrics optimized by each algorithm are selected as final sensor locations, as shown in Figs 9 to 14. Apart from the ADPR algorithm, this approach enables better distribution of the sensors

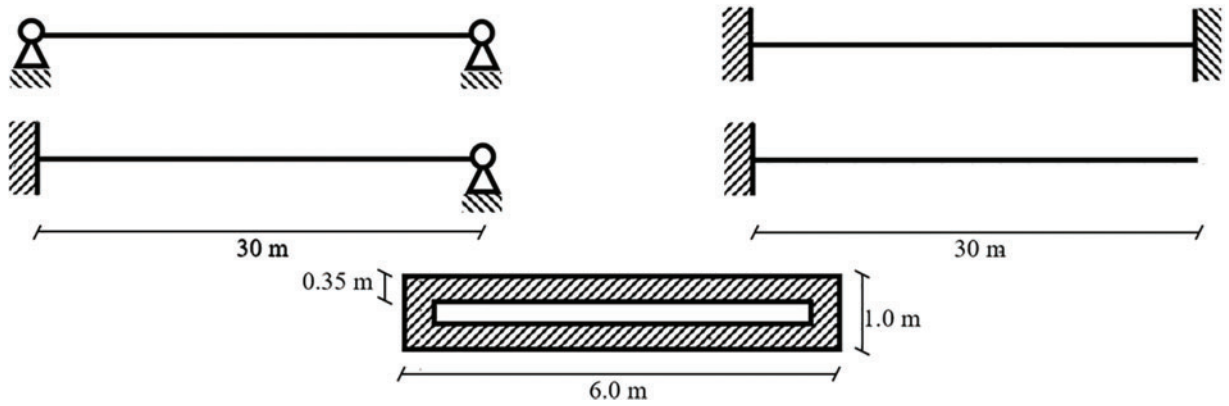

Figure 1. Geometry of the beam structures used in the analytical examples

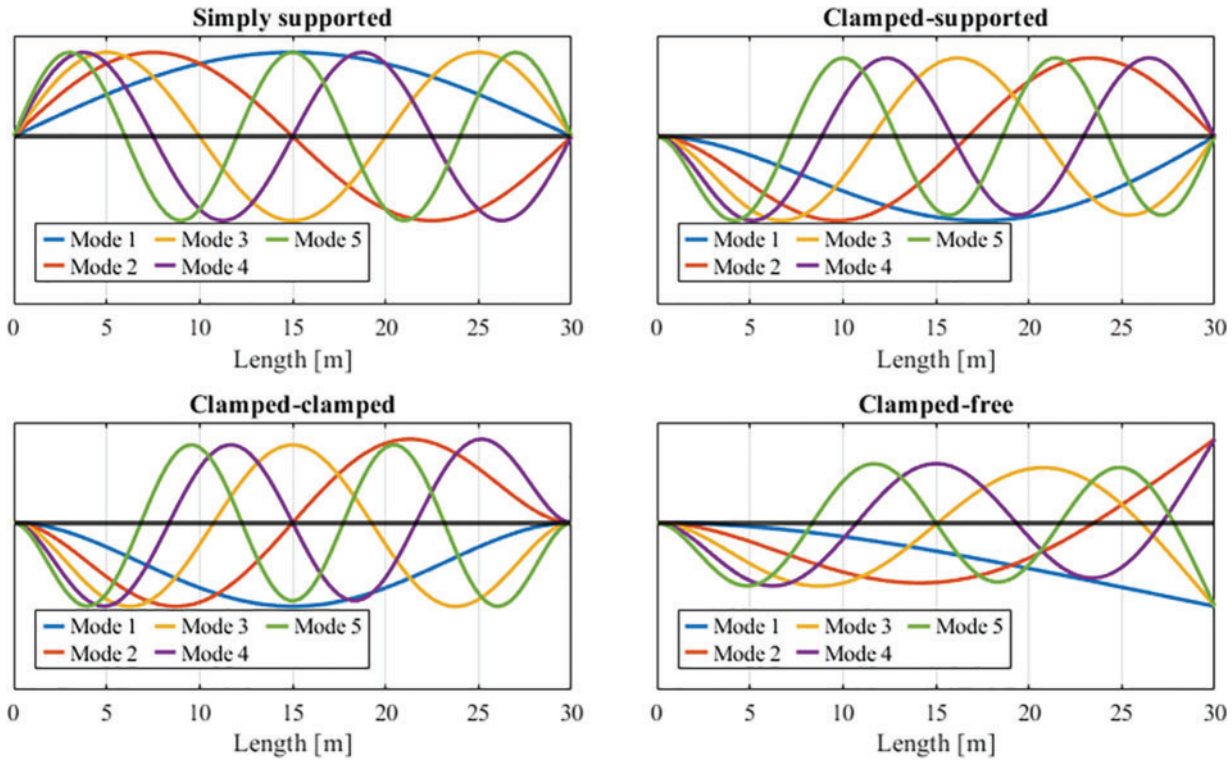

Figure 2. First five mode shapes of the investigated concrete beams

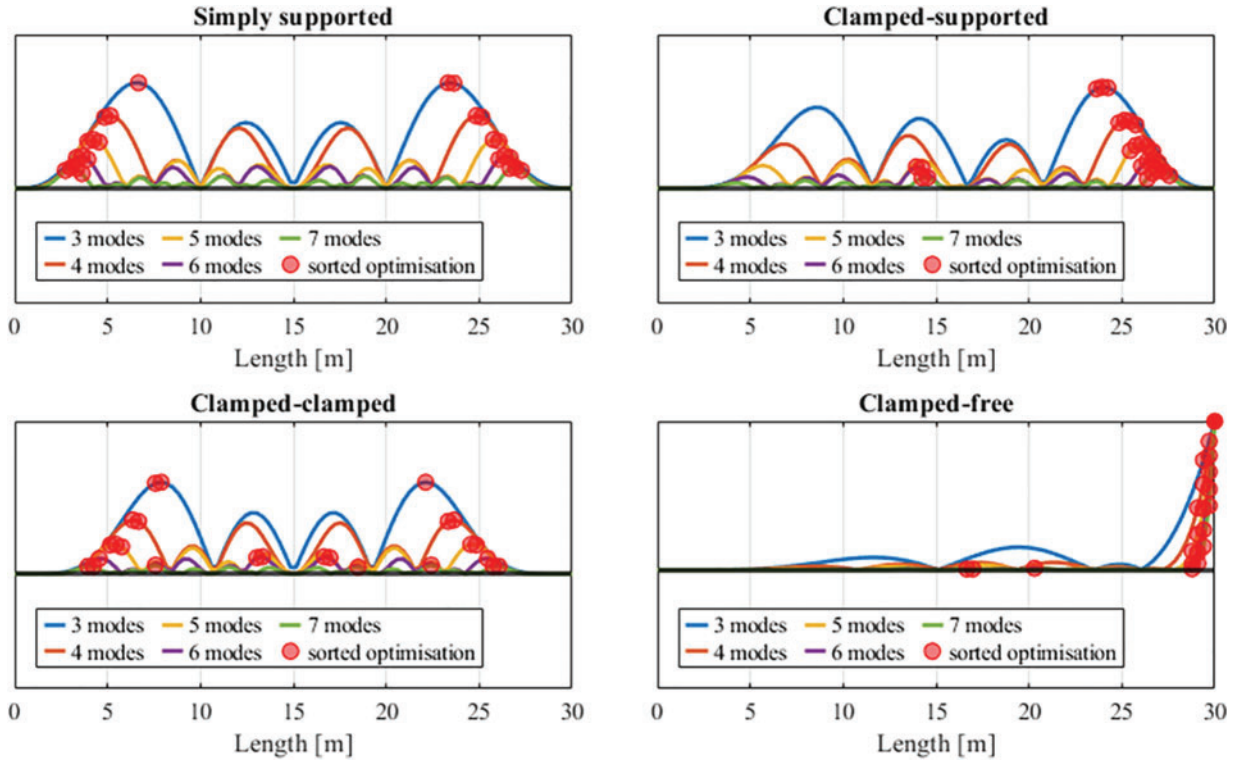

Figure 3. Spatial variation of the EVP function with identification of the optimal sensor locations

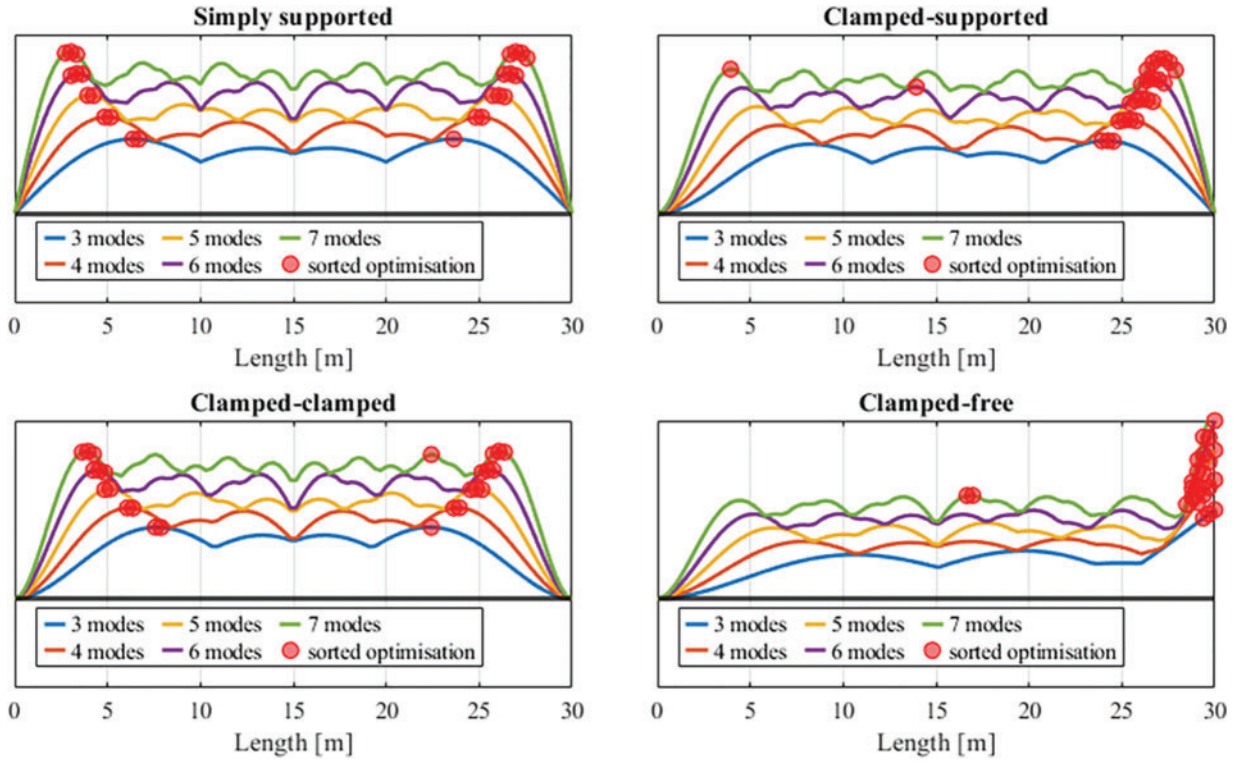

Figure 4. Spatial variation of the MSSP function with identification of the optimal sensor locations

throughout the structure, avoiding blind spots or areas with insufficient data coverage to adequately capture the modal behavior of the system across different configurations. While in the standard approach, the number of sensors is equal to the target modes, this approach determines a variable number of sensors corresponding to the local maxima of the metric functions, providing an estimate of the optimal number of sensors to install.

For better visualization of the results, Fig. 15 illustrates the final sensor placements derived from the investigated

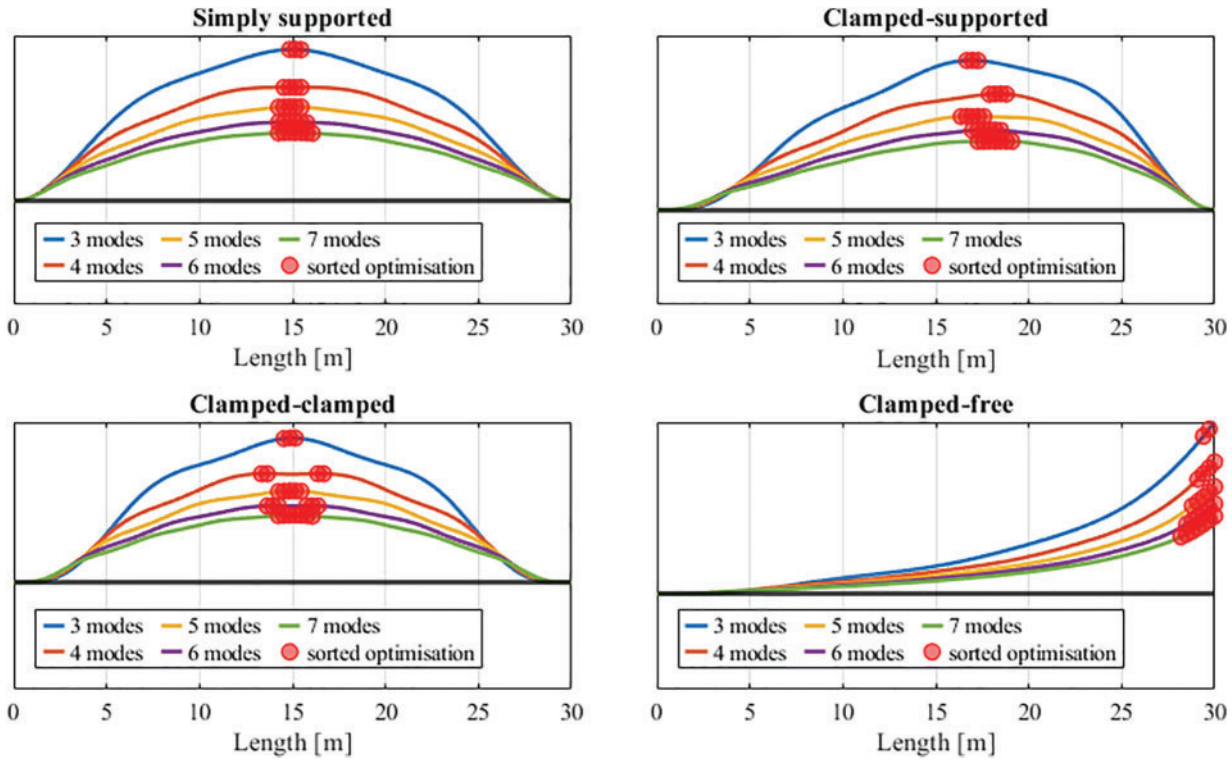

Figure 5. Spatial variation of the ADPR function with identification of the optimal sensor locations

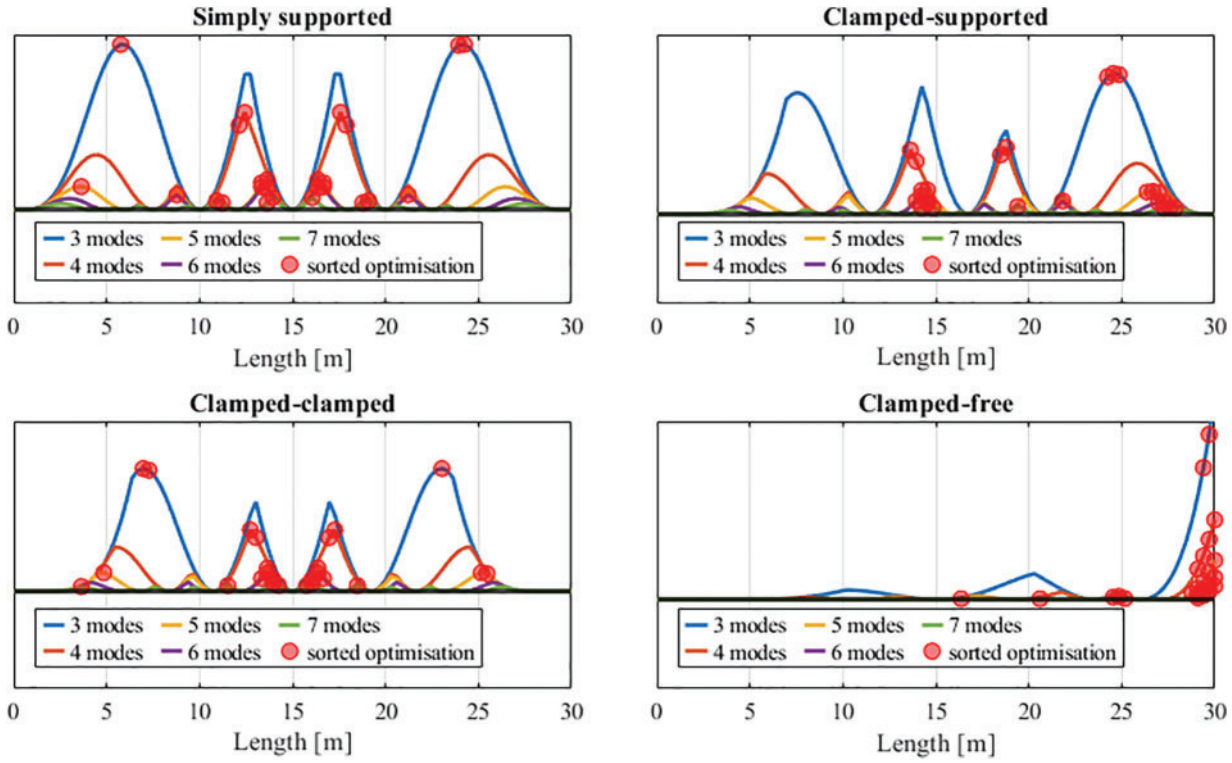

Figure 6. Spatial variation of the WDPR function with identification of the optimal sensor locations

OSP algorithms, enhanced by the local maxima selection, for the simply supported beam in cases of 3, 4, or 5 target modes. It is noted that many locations, that is, local maxima in the metric functions, are commonly identified as optimal by different methods, particularly MSSP, EVP, NODP, and WDPR. As expected from their formulations, these methods tend to reject near-nodal regions of the target modes, such as the mid-span, even though this point exhibits the maximum modal displacement for other target modes. Regarding the other algorithms, the ADPR appears

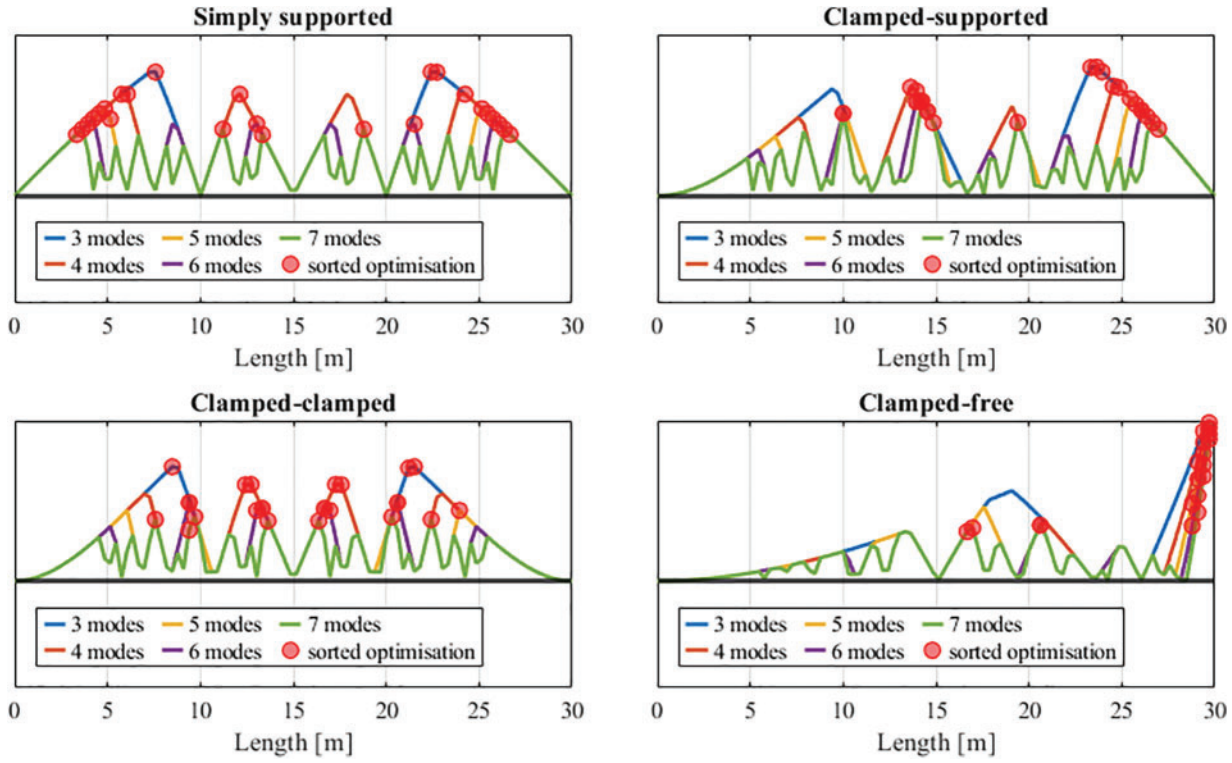

Figure 7. Spatial variation of the NODP function with identification of the optimal sensor locations

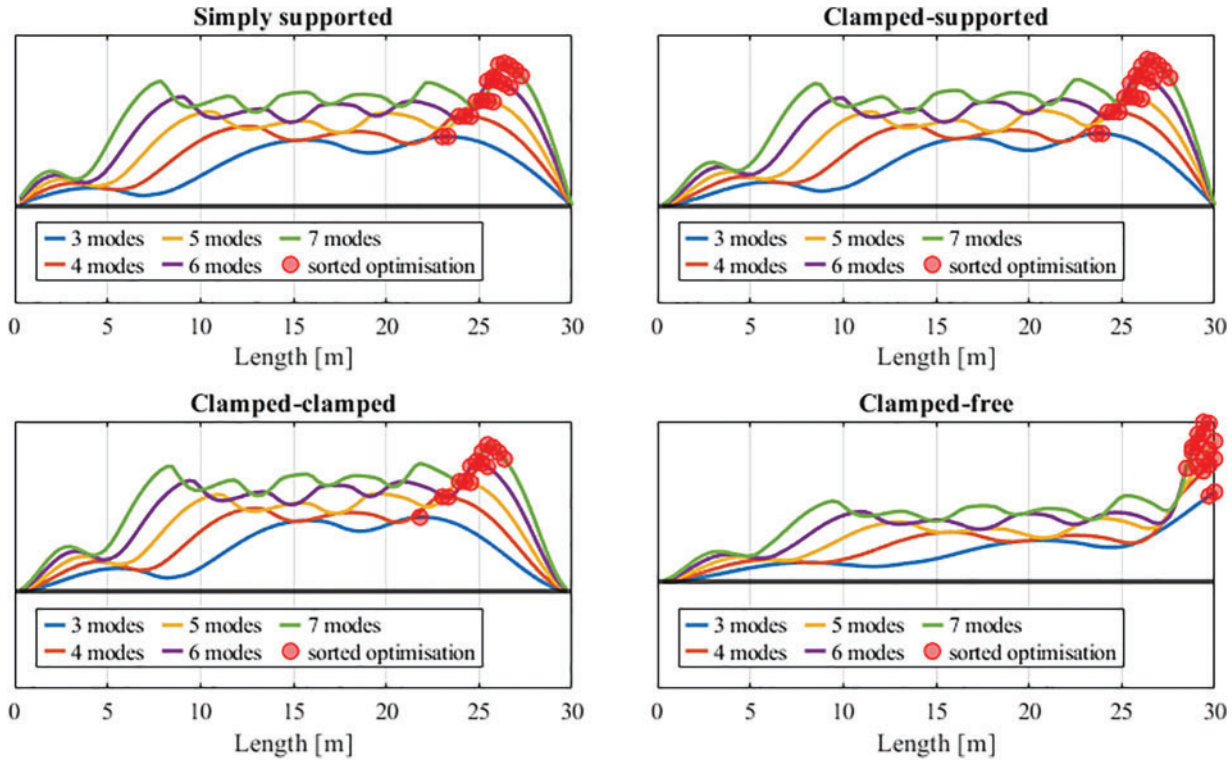

Figure 8. Spatial variation of the VM function with identification of the optimal sensor locations

inconclusive, while the VM method yields a solution closely aligned with those provided by the QRD and EfI methods, presented here as benchmarks for the enhanced approaches. It is worth stressing that the local maxima approach generally identifies more necessary sensors than the number of target modes, which has significant implications in terms of both the cost and complexity of the SHM sensor network. An increased number of sensors can lead to higher expenses for installation, maintenance, and data management. The added complexity may also require more sophisticated data

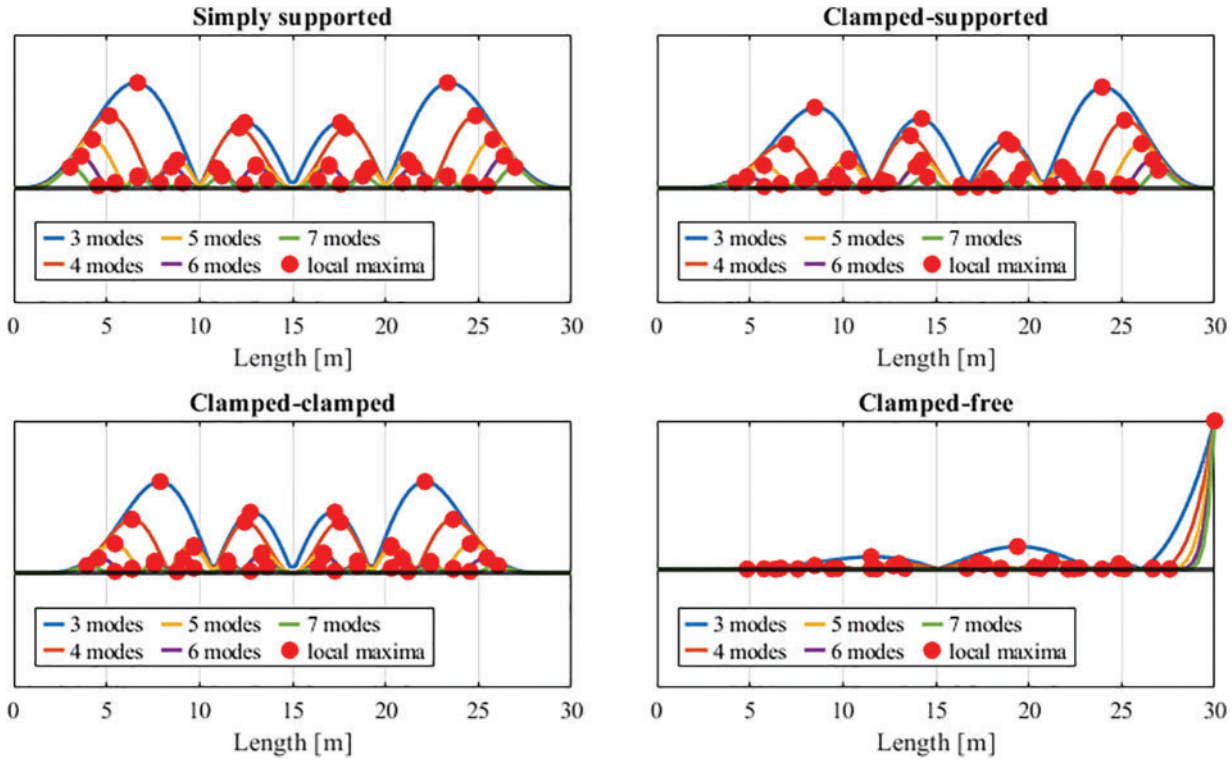

Figure 9. Spatial variation of the EVP function with identification of the optimal sensor locations based on local maxima

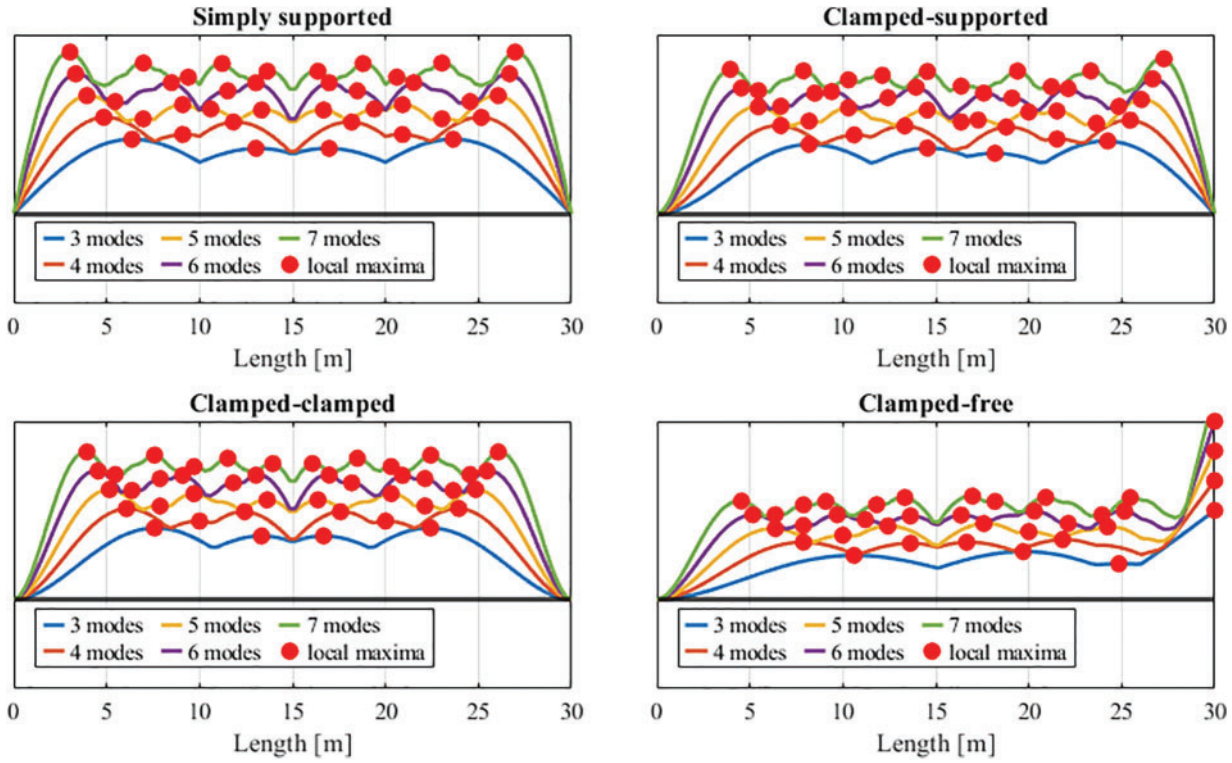

Figure 10. Spatial variation of the MSSP function with identification of the optimal sensor locations based on local maxima

analysis and integration methods to effectively process and interpret the sensor data. Notably, for this specific case, the number of required sensors increases significantly when selecting five or more target modes, as shown in Table 1. This is because incorporating additional modes into the metric functions produces more local optima. Among all the analyzed heuristics, the VM method appears to be the only

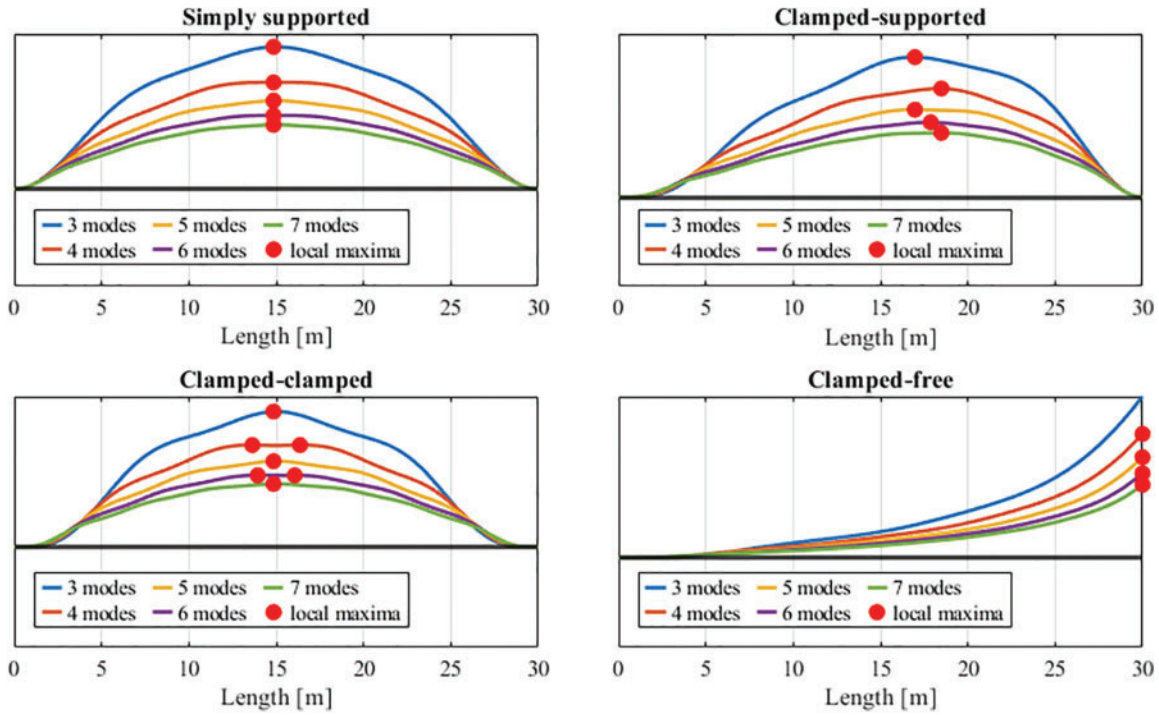

Figure 11. Spatial variation of the ADPR function with identification of the optimal sensor locations based on local maxima

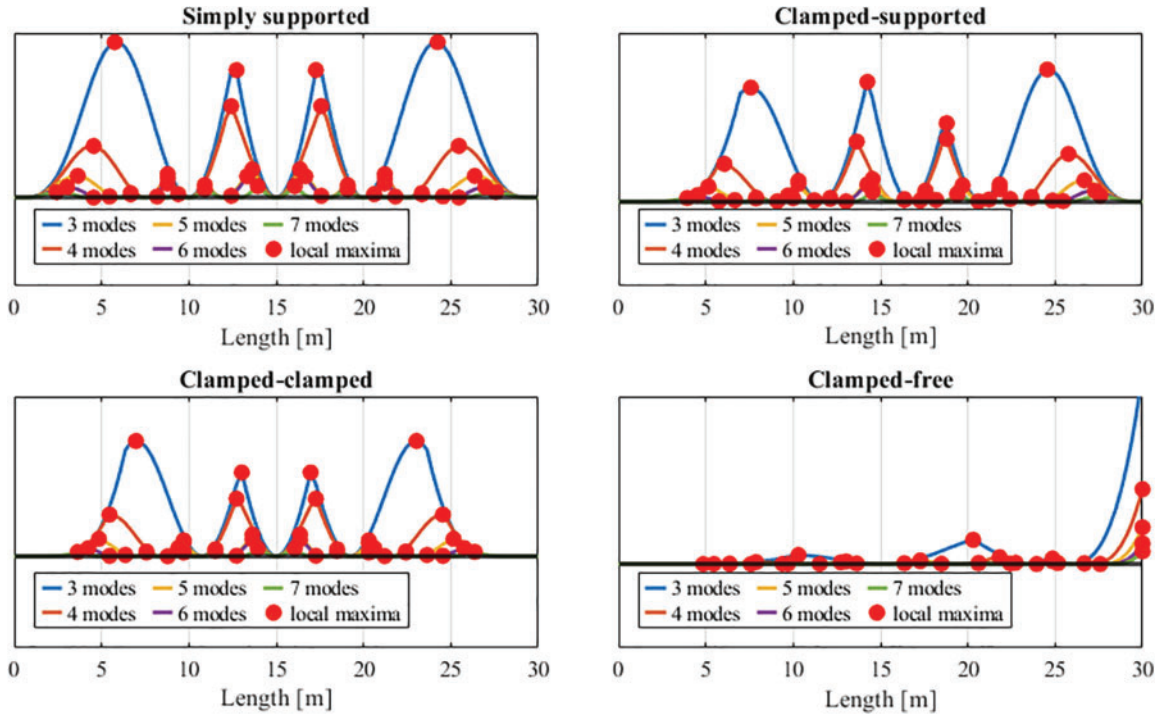

Figure 12. Spatial variation of the WDPR function with identification of the optimal sensor locations based on local maxima

one able to provide an optimized network with a minimum number of sensors.

To further assess the performance of the algorithms, the average values of the off-diagonal terms of the AutoMAC matrix, obtained by comparing the mode shapes estimated through the reduced sensor configurations derived from each algorithm, are evaluated. It is well known that high values of the off-diagonal AutoMAC terms indicate similarity or overlap between modal vectors, which can hinder the accurate identification of the structure's dynamic behavior. Conversely, off-diagonal MAC terms close to zero indicate orthogonality and linear independence between mode

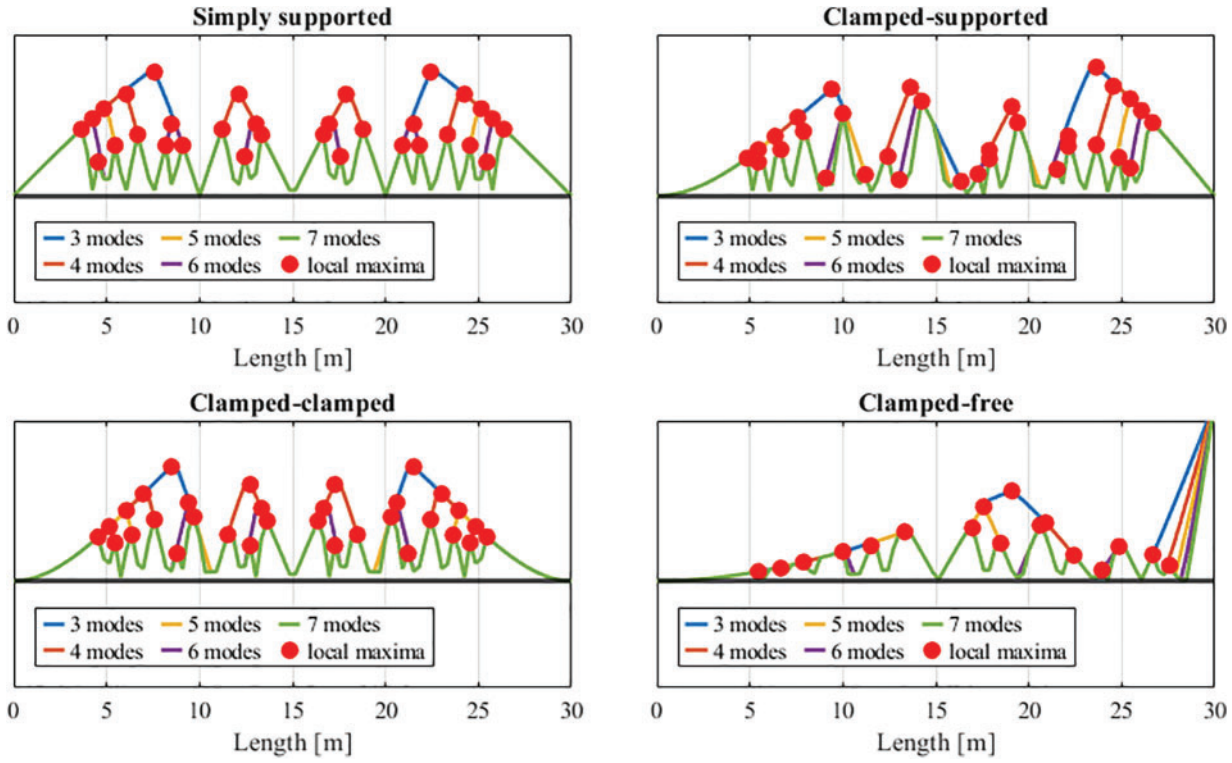

Figure 13. Spatial variation of the NODP function with identification of the optimal sensor locations based on local maxima

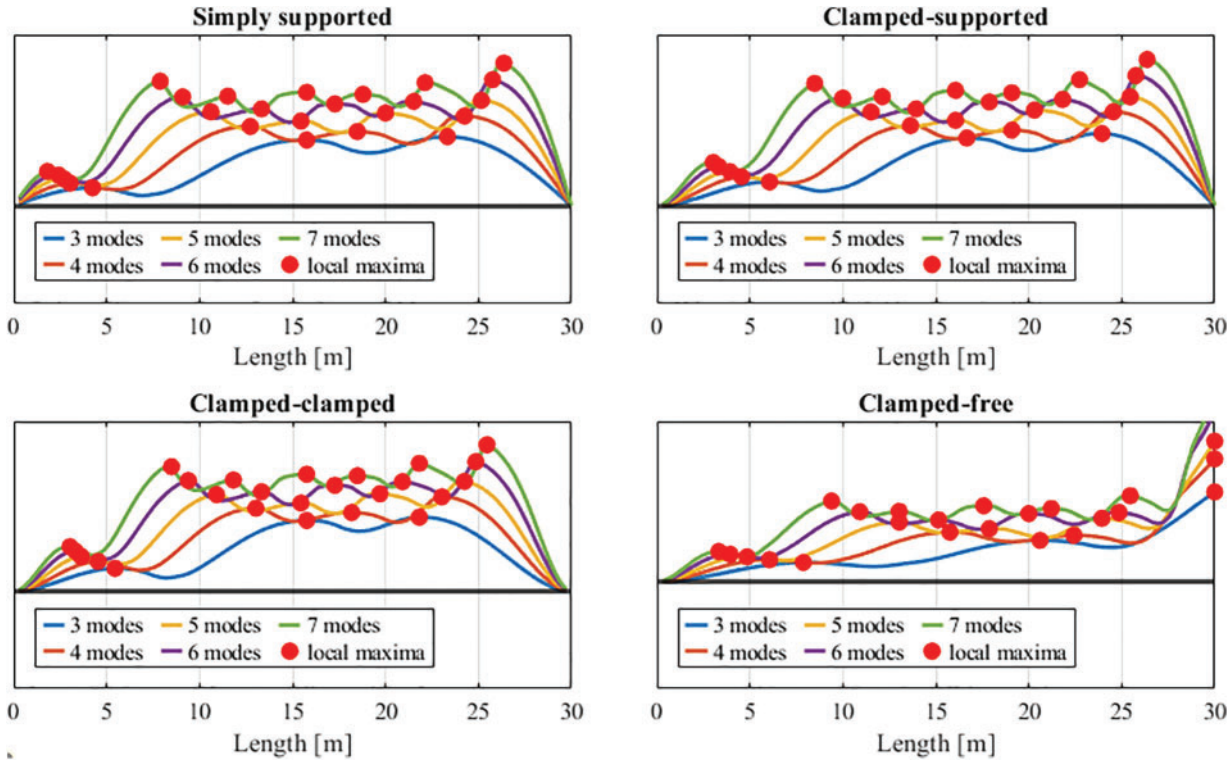

Figure 14. Spatial variation of the VM function with identification of the optimal sensor locations based on local maxima

shapes. Maintaining low off-diagonal values is particularly important for SHM applications, where the ability to distinguish between modes directly impacts the precision of damage detection and dynamic response predictions. As an example, Table 2 reports the average AutoMAC off-diagonal terms for the simply supported case. The results demonstrate that by employing the local maxima approach, all single-iteration heuristics—except for the ADPR algorithm—yield

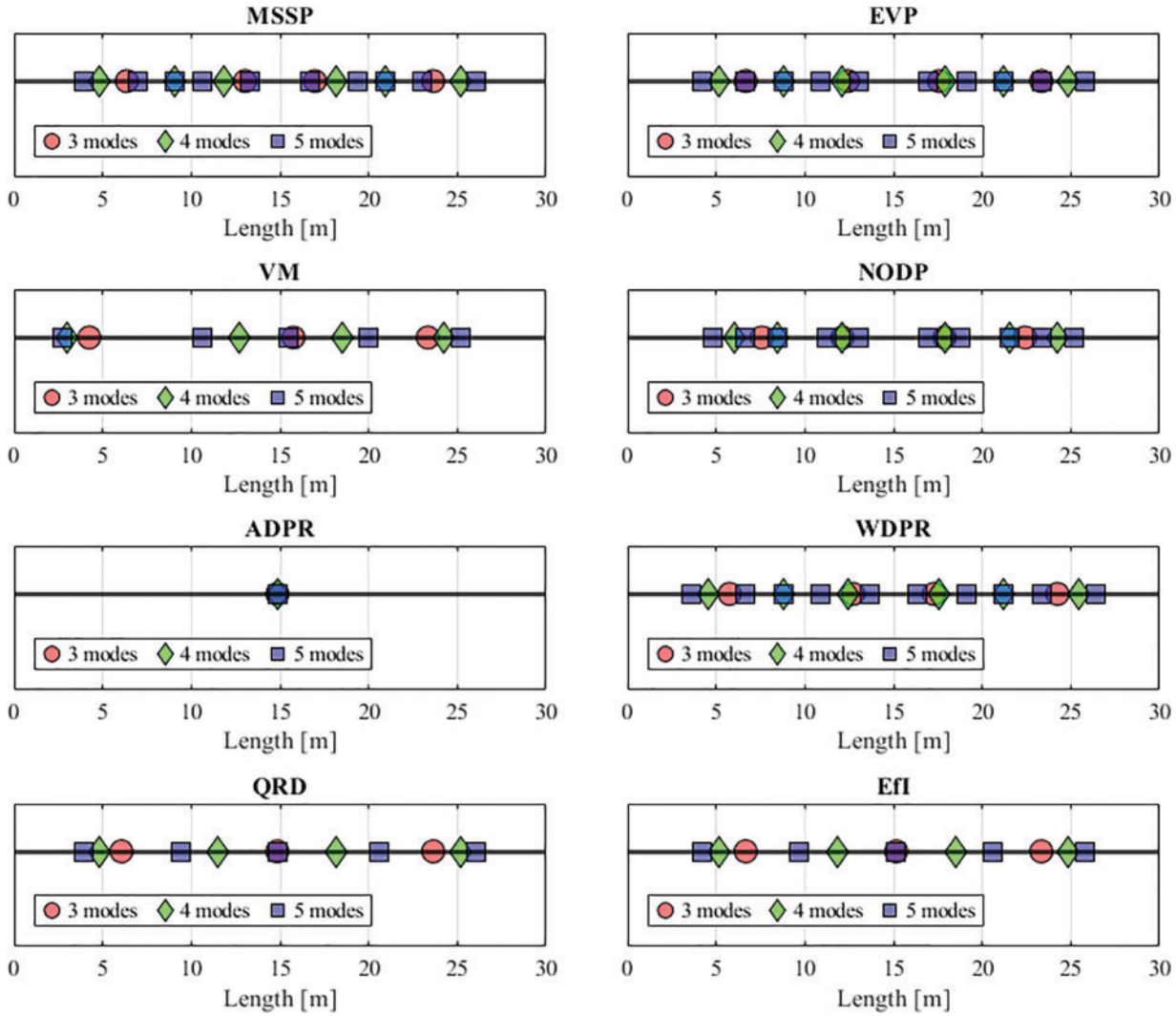

Figure 15. Best sensor placements achieved by the investigated heuristics with an increasing number of target modes (case study: simply supported beam)

Table 1. Number of optimal sensor locations (local maxima) in the investigated metric functions modes (case study: simply supported beam)

Modes	MSSP	EVP	VM	NODP	ADPR	WDPR
3	4	4	3	4	1	4
4	6	6	4	6	1	6
5	10	10	5	10	1	10
6	10	12	6	12	1	12
7	10	18	7	18	1	18

sensor configurations that ensure the accurate identification of linearly independent mode shapes, significantly enhancing the performance of the standard approach. This is evidenced by the fact that the average value of the off-diagonal MAC terms is consistently close to zero, even when the number of target modes increases. Except for ADPR, VM exhibits a slightly higher average of the off-diagonal terms; however, this method requires fewer sensors to achieve a similar performance. Overall, the local optima approach improves the performance of the individual sensor ranking methods, making them comparable to the EfI and QRD methods. Both of these latter methods show excellent performance while requiring, in some cases, only half the sensors used by the competing algorithms, confirming their robustness and reliability in the context of OSP.

The findings discussed above are further corroborated by examining the CrossMAC values between the complete mode shape matrix and the expanded mode shape matrix

reconstructed through spline interpolation based on the optimal sensor locations, as shown in Table 3 for the same instance. In this case, diagonal terms as close as possible to one are desired, as they indicate a strong correspondence between the modal vectors estimated by the extensive sensor network and those estimated by the reduced one,

Table 2. Average AutoMAC off-diagonal terms for the simply supported beam

No. target modes	Single-iteration heuristics													
	Standard approach						Local maxima approach							
	MSSP	EVP	VM	NODP	ADPR	WDPR	MSSP	EVP	VM	NODP	ADPR	WDPR	QRD	EfI
3	0.27	0.27	0.67	0.27	0.34	0.27	0.01	0.00	0.02	∼0.0	0.67	∼0.0	∼0.0	∼0.0
4	0.25	0.25	0.74	0.12	0.25	0.25	0.01	0.01	0.02	0.01	0.75	∼0.0	∼0.0	∼0.0
5	0.34	0.34	0.78	0.33	0.37	0.18	0.01	0.01	0.01	0.01	0.80	∼0.0	∼0.0	∼0.0
6	0.33	0.33	0.79	0.11	0.33	0.12	∼0.0	0.01	0.01	0.01	0.83	∼0.0	∼0.0	∼0.0
7	0.37	0.37	0.77	0.11	0.39	0.20	0.01	0.01	0.01	0.01	0.86	∼0.0	∼0.0	∼0.0

Table 3. CrossMAC values between reconstructed and complete mode shapes for the simply supported beam

MSSP	EVP	VM	NODP	ADPR	WDPR	QRD	EfI
			3 modes				
1.00	1.00	1.00	1.00	1.00	1.00	1.00	1.00
1.00	1.00	0.98	1.00	0.00	1.00	0.98	0.98
0.97	0.97	0.97	0.96	0.00	0.97	0.98	0.98
			4 modes				
1.00	1.00	1.00	1.00	1.00	1.00	1.00	1.00
1.00	1.00	1.00	1.00	0.00	1.00	1.00	1.00
1.00	1.00	0.94	0.99	0.00	1.00	0.96	0.96
0.98	0.98	0.97	0.97	0.00	0.98	0.98	0.98
			5 modes				
1.00	1.00	1.00	1.00	1.00	1.00	1.00	1.00
1.00	1.00	1.00	1.00	0.00	1.00	1.00	1.00
1.00	1.00	0.99	1.00	0.00	1.00	0.99	0.99
1.00	1.00	0.94	0.99	0.00	1.00	0.94	0.94
0.98	0.98	0.96	0.98	0.00	0.99	0.98	0.98
			6 modes				
1.00	1.00	1.00	1.00	1.00	1.00	1.00	1.00
1.00	1.00	1.00	1.00	0.00	1.00	1.00	1.00
1.00	1.00	1.00	1.00	0.00	1.00	1.00	1.00
1.00	1.00	0.97	1.00	0.00	1.00	0.99	0.98
0.99	0.99	0.95	0.99	0.00	1.00	0.92	0.93
0.98	0.99	0.92	0.98	0.00	0.99	0.98	0.98
			7 modes				
1.00	1.00	1.00	1.00	1.00	1.00	1.00	1.00
1.00	1.00	1.00	1.00	0.00	1.00	1.00	1.00
1.00	1.00	1.00	1.00	0.00	1.00	1.00	1.00
1.00	1.00	0.99	1.00	0.00	1.00	1.00	1.00
0.99	1.00	0.96	1.00	0.00	1.00	0.98	0.98
0.98	1.00	0.96	0.99	0.00	1.00	0.90	0.91
0.99	0.99	0.86	0.98	0.00	0.99	0.98	0.98

suggesting that the optimized sensor locations provide a reliable reconstruction of the mode shapes at unmeasured nodes. As observed, the diagonal values of CrossMAC remain close to one for all heuristics except for the ADPR algorithm. This indicates that the reduced sensor configurations derived from the analyzed techniques successfully capture the original mode shapes with minimal loss of information. Moreover, their performance is not compromised as the number of target modes increases, demonstrating the robustness and adaptability of these heuristics. Similar observations apply to the other instances, which are omitted here for brevity.

Application to a Multi-Span Concrete Bridge

The different OSP techniques analyzed in the previous section are applied to a real large-scale bridge, specifically the Z24. The choice of such a well-known experimental benchmark as a testbed lies in the possibility to exploit an unprecedented number of vibration signatures from a real-world case study under both normal and abnormal conditions. This enables the assessment of the applicability and reliability of established OSP algorithms in engineering practice.

Description of the experimental benchmark

The Z24 bridge, built in Switzerland in the 1960s, was an overpass of the A1 Bern–Zurich highway linking the villages of Koppigen and Utzenstorf. It was a typical continuous post-tensioned concrete girder bridge with a total length of 58 m, subdivided into three spans of approximately 14, 30, and 14 m, respectively (Fig. 16). To protect the anchor heads, both ends of the deck were extended by an additional 2.7 m each. From a static standpoint, the bridge consisted of a two-cell box girder superstructure rigidly supported by two intermediate concrete diaphragms as main piers, while the abutments rested on triplets of columns pinned at both ends. Supports were rotated with respect to the longitudinal axis of the deck, yielding a slightly oblique bridge. The condition of the infrastructure was relatively good, yet the construction of a new railway track adjacent to the highway made its demolition and subsequent replacement necessary. Before this occurred, within the framework of the SIMCES research project,[26] the structure was subjected to progressive damage tests to demonstrate the possibility of identifying structural damage from changes in the dynamic characteristics estimated from the bridge vibration measurements prior to and after each damage scenario (DS). To this end, forced and ambient input excitations were employed to collect the response of a very large number of degrees of freedom (291 DOFs in total) through a dense sensor network of cabled accelerometers. The measurement points were distributed both on top of the bridge deck (along three parallel lines of 45 points each) and on the main pillars (along two parallel lines of 8 points each), as shown in Fig. 16. Nine setups and three reference channels were necessary to collect the response from such a dense measurement grid.

For each test, output vibration signals were acquired for about 11 minutes with a sampling rate of 100 Hz to capture all frequencies of interest for the bridge. A detailed description of the entire experimental campaign, along with the sequence and extent of the various DSs, is provided in.[27–29] For the purpose of this work, one reference scenario (RS) representative of the undamaged condition of the bridge and two DSs corresponding to realistic and relevant cases of structural damage are considered, namely: (1) settlement of the Koppigen pier foundation at 44 m (DS_1), and (2) failure of the concrete hinges at the abutments (DS_2). Possible variations induced by changing

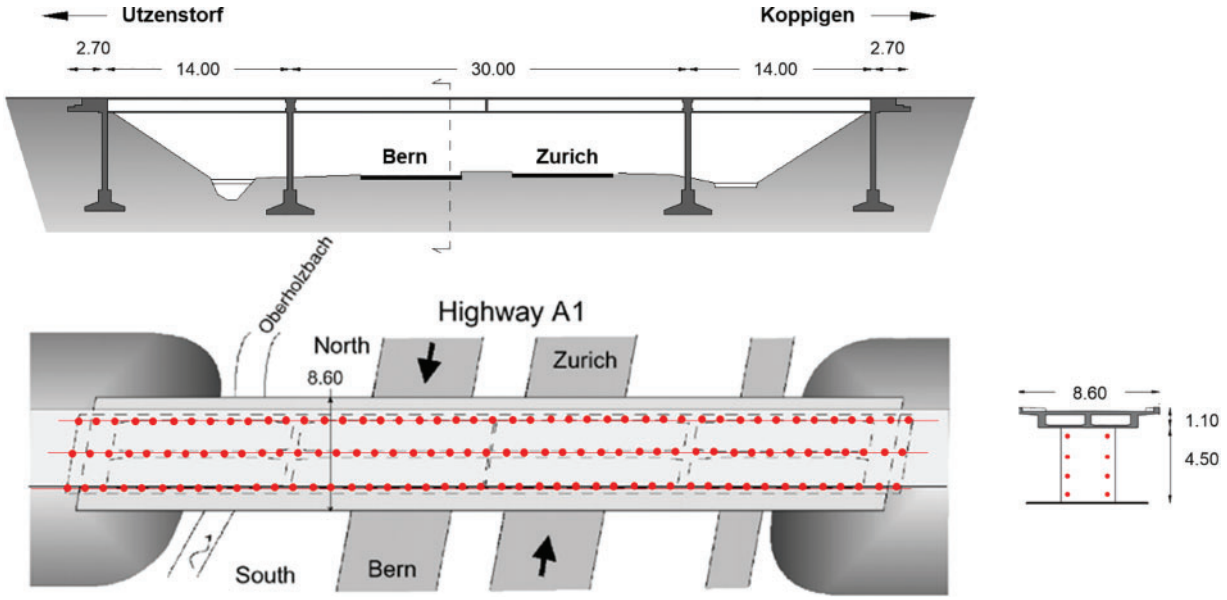

Figure 16. Geometry of the Z24 bridge and distribution of measurement points for the AVT (adapted from[12]) (Dimension in meters)

ambient parameters—commonly considered in long-term bridge monitoring—are not accounted for in this study, as the analyzed data were collected from multi-setup ambient vibration tests carried out over a short time period. As a result, environmental adjustments were not required.

Modal feature extraction for different DSs

To characterize the dynamics of the bridge, modal parameters were extracted by processing the nodal responses experimentally collected from the central array of sensors deployed on top of the deck using the Enhanced Frequency Domain Decomposition algorithm implemented in ARTeMIS software. A total of 108 channels (45 in the vertical direction, 45 in the transversal direction, and 18 in the longitudinal direction) was considered to realistically reproduce sensor networks of high spatial density.

Five vibration modes were identified within the frequency range of 0–15 Hz (Fig. 17): the first mode corresponds to the fundamental bending mode of the bridge, the second is a transverse mode with dominant lateral components, the third and fourth are asymmetric double-curvature bending modes coupled with torsional motions, and the fifth is a pure symmetric bending mode with greater modal deflections at the side spans. Fig. 18 shows the configuration of the estimated experimental modes of the Z24 bridge, along with their frequencies (f) and damping ratios (ξ) for the

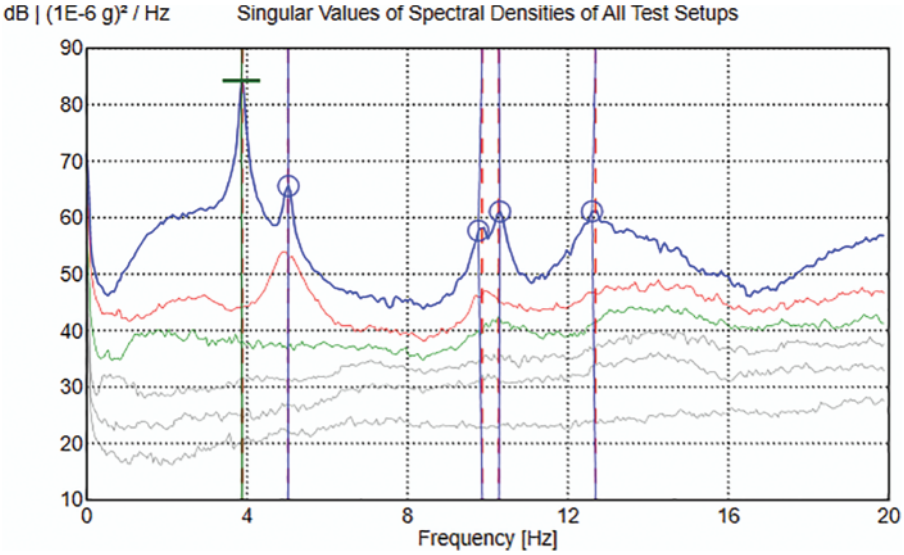

Figure 17. Singular value decomposition of spectral densities obtained from the 108-channel sensor configuration

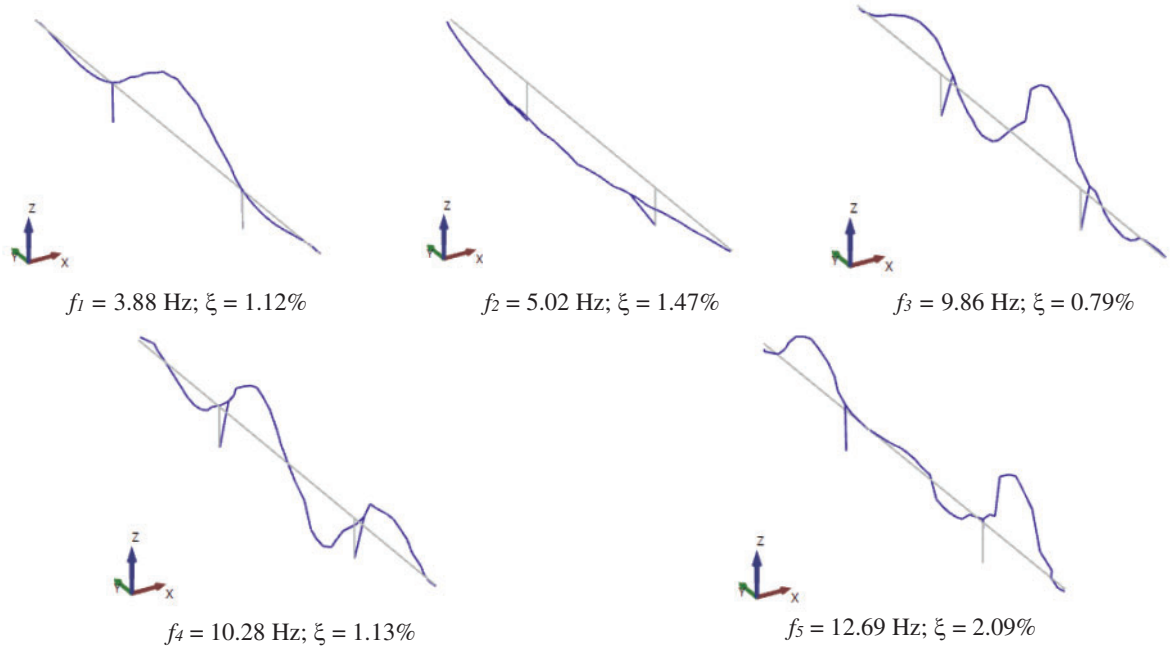

Figure 18. Main vibration modes of the Z24 bridge identified with the full sensor configuration (108 channels) in the reference scenario

RS. Note that all vertical modes show an increasing number of inflection points as well as a growing amount of modal complexity, making them progressively more sensitive to deflection changes originating from local damage phenomena.

The modal feature extraction process with the full 108-channel dataset is repeated for all investigated structural conditions, namely RS, DS_1, and DS_2, assuming all DSs as equally possible. The outcome is summarized in Table 4. The frequency difference (Δf) and degree of consistency (MAC) between mode pairs of damage and reference scenarios are also reported. It can be observed that damage-induced stiffness variations are clearly reflected by changes in the modal parameters, with frequency average downshifts of nearly 4.6% and 3.5% for DS_1 and DS_2, respectively, and MAC values <0.85 for modes 3, 4, and 5 in both DSs. It is worth noting that the greater the number of inflection points featured by the mode shapes, the greater their sensitivity to damage-induced deflection changes, and the lower their degree of similarity with respect to the undamaged counterparts.

Definition of a modal-based multi-criteria optimization approach

One of the most critical aspects when dealing with heuristic OSP approaches is the establishment of well-defined criteria to guide the selection of the optimal candidate solution among various, apparently equivalently efficient alternatives. These criteria must prioritize maximizing modal information across multiple scenarios, as structural systems evolve over time and sensor networks cannot be designed solely based on baseline conditions. This consideration is particularly important for ensuring the adaptability and robustness of the sensor placement strategy in the face of changing structural behaviors. Taking these aspects into account, along with the outcomes obtained from the analytical examples discussed in Section 3, specific evaluation criteria are formulated to compare the performance of the investigated OSP techniques and to drive the selection of the optimal sensor configuration for the Z24 bridge. These criteria are outlined as follows:

1) Maximization of the number of identified modes with frequency error <1% in the reduced sensor configuration: To design a cost-efficient sensor placement, as many critical modes as possible must be monitored with a limited number of sensors. Therefore, maximizing the number of modes that can be identified with a small error margin in terms of frequencies ensures that important vibrational characteristics are accurately captured.

2) Minimization of average frequency error between corresponding modes estimated through the full and reduced set of sensors: When comparing the modes identified using the reduced (optimized) sensor configuration to those from a more refined setup (e.g., a dense sensor network), the frequency error must be minimized to ensure that the modes closely match the true modal frequencies of the structure.

3) Minimization of the average value of the off-diagonal terms of the AutoMAC matrix obtained per each candidate sensor configuration: High values of off-diagonal MAC terms indicate hardly distinguishable mode shapes. By minimizing these values, the sensor configuration is optimized to reduce mode shape overlap and redundancy, ensuring that each sensor contributes unique and independent dynamic information.

4) Minimization of the distance between corresponding mode shapes of the full and reduced sensor configurations: Minimizing the degree of dissimilarity (calculated as 1 – MAC) between modes ensures that mode shapes identified in the reduced configuration closely resemble those estimated from the full configuration. Accurately capturing mode shapes is critical for tasks such as damage detection.

5) Maximization of the ratio between diagonal covariance coefficients and the sum of their off-diagonal terms: The diagonal terms of the covariance matrix of the mode shape matrix represent the energy associated with each mode, while the off-diagonal terms reflect how much the modes interfere or overlap with each other. The higher the ratio of diagonal to off-diagonal terms, the stronger each mode's contribution.

6) Identification of recurrent sensor locations: The repeated appearance of specific sets of sensors across multiple near-optimal configurations, as well as across different scenarios, indicates their consistently high contribution to capturing critical structural information.

Table 4. Frequencies and damping ratios of the Z24 bridge estimated with the full sensor layout (108 channels) across different scenarios

Mode	RS		DS1				DS2			
	f (Hz)	ξ (%)	f (Hz)	ξ (%)	Δf (%)	MAC	f (Hz)	ξ (%)	Δf (%)	MAC
1	3.88	1.12	3.69	1.16	−4.90	1.00	3.85	1.14	−0.77	1.00
2	5.02	1.47	4.92	1.82	−1.99	0.96	4.69	1.67	−6.57	0.97
3	9.86	0.79	9.27	0.88	−5.98	0.75	9.75	0.96	−1.12	0.53
4	10.28	1.13	9.66	1.17	−6.03	0.82	10.18	1.04	−0.97	0.81
5	12.69	2.09	12.19	2.22	−3.94	0.70	11.71	2.17	−7.72	0.61
Avg	–	1.32	–	1.45	−4.57	–	–	1.40	−3.43	–

The optimal sensor configuration is the one that best satisfies the established criteria in the majority of the considered scenarios, ensuring minimal overlap between mode shapes and maximizing the clarity and distinctiveness of the captured dynamic information.

Comparison of investigated OSP techniques

To achieve the dual goal of maximizing SHM information while minimizing equipment installation and maintenance costs, the eight optimization algorithms presented in Section 2 and analyzed in Section 3 are applied using their standard formulation to obtain a reduced set of sensors as informative as possible for the investigated bridge, accounting for different conditions associated with the occurrence of potential structural damage. The problem's dimensionality is reduced from 108 to 5 degrees of freedom, which represent the minimum number necessary to identify the primary five vibration modes of the bridge with sufficient accuracy while avoiding inconsistent solutions. The eight candidate sensor configurations derived from the applied OSP techniques are depicted in Fig. 19, highlighting the position and direction of each channel. As expected, sub-optimal solutions vary among different methods, yet most of the channels are identified as best by the majority of the algorithms.

Tables 5–7 give a comparative insight into the modal frequency results obtained per each scenario from the sub-optimal reduced sets of sensors (5 DOFs) with respect to those obtained from the full sensor configuration (108 DOFs). Looking at the frequency percentage error, it is found that the candidate sensor configuration identified from the MSSP technique (i.e., OSP3) is the best in the RS. On the other hand, the sensor configuration commonly identified from EVP, WDPR, and NODP techniques, namely OSP2/OSP5/OSP8, or the configurations derived from the ADPR and VM methods, that is, OSP4 and OSP7, appear to be the optimal solutions to catch potential damages.

For a better assessment of the reliability and sensitivity of the different OSP techniques, considerations are also extended to the mode shapes by comparing the average of the off-diagonal terms of the AutoMAC matrices estimated for

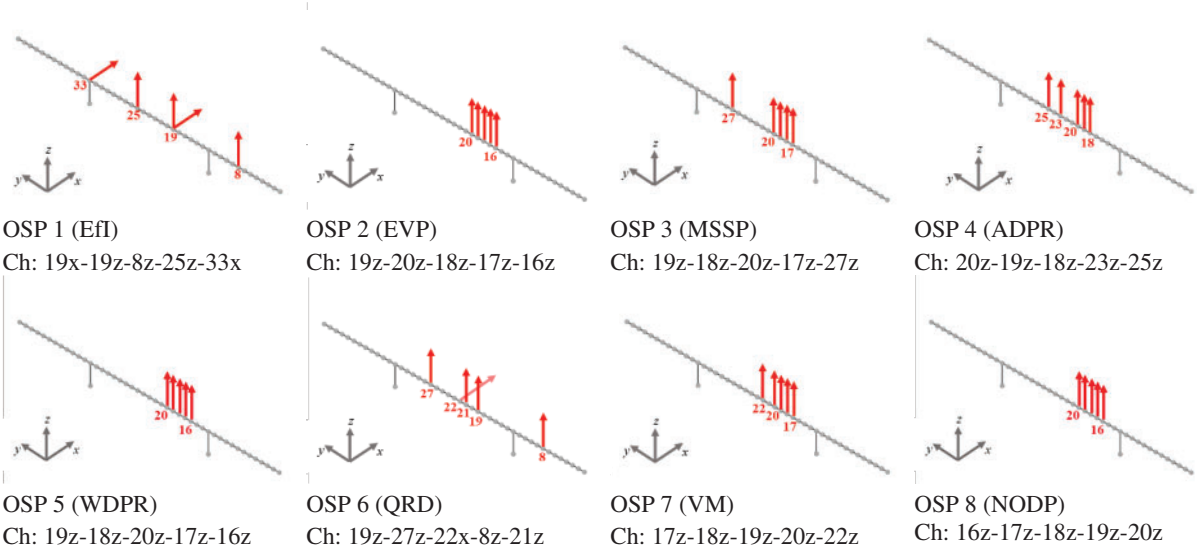

Figure 19. Heuristic-based candidate sensor configurations for the Z24 bridge. Algorithm acronyms are indicated between parentheses (EVP, WDPR, and NODP yield the same OSP)

Table 5. Frequency values of the vibration modes estimated from the candidate OSP configurations in the reference scenario (RS). Average frequency percentage error and number of identified modes with $\Delta f < 1\%$ are highlighted in bold

RS	OSP1		OSP2|OSP5|OSP8		OSP3		OSP4		OSP6		OSP7	
	EfI		EVP|WDPR|NODP		MSSP		ADPR		QRD		VM	
Mode	f (Hz)	$\lvert\Delta f\rvert$(%)	f (Hz)	$\lvert\Delta f\rvert$(%)	f (Hz)	$\lvert\Delta f\rvert$(%)	f (Hz)	$\lvert\Delta f\rvert$(%)	f (Hz)	$\lvert\Delta f\rvert$(%)	f (Hz)	$\lvert\Delta f\rvert$(%)
1	3.87	0.26	3.88	0.00	3.88	0.00	3.87	0.26	3.87	0.26	3.87	0.26
2	5.03	0.20	5.03	0.20	5.03	0.20	5.03	0.20	5.04	0.40	5.03	0.20
3	9.91	0.51	9.81	0.51	9.84	0.20	9.85	0.10	9.82	0.41	9.88	0.20
4	10.24	0.39	10.32	0.39	10.3	0.19	10.29	0.10	10.29	0.10	10.29	0.10
5	12.60	0.71	12.74	0.39	12.76	0.55	12.79	0.79	13.17	3.78	12.78	0.71
Avg	–	**0.41**	–	**0.30**	–	**0.23**	–	**0.29**	–	**0.99**	–	**0.29**
$M_{(\Delta f<1\%)}$	–	**5**	–	**5**	–	**5**	–	**5**	–	**4**	–	**5**

Table 6. Frequency values of the vibration modes estimated from the candidate OSP configurations in the first damage scenario (DS_1). Average frequency percentage error and number of identified modes with $\Delta f<1\%$ are highlighted in bold

DS_1	OSP1		OSP2|OSP5|OSP8		OSP3		OSP4		OSP6		OSP7	
	EfI		EVP|WDPR|NODP		MSSP		ADPR		QRD		VM	
Mode	f (Hz)	$\|\Delta f\|$(%)	f (Hz)	$\|\Delta f\|$(%)	f (Hz)	$\|\Delta f\|$(%)	f (Hz)	$\|\Delta f\|$(%)	f (Hz)	$\|\Delta f\|$(%)	f (Hz)	$\|\Delta f\|$(%)
1	3.69	0.00	3.69	0.00	3.69	0.00	3.69	0.00	3.69	0.00	3.69	0.03
2	4.92	0.00	4.92	0.00	4.93	0.20	4.93	0.20	4.92	0.00	4.92	0.08
3	9.34	0.76	9.25	0.22	9.23	0.43	9.24	0.32	9.23	0.43	9.24	0.32
4	9.66	0.00	9.69	0.31	9.69	0.31	9.7	0.41	9.68	0.21	9.70	0.37
5	12.49	2.46	12.18	0.08	12.11	0.66	12.17	0.16	12.43	1.97	12.16	0.21
Avg	–	**0.64**	–	**0.12**	–	**0.32**	–	**0.22**	–	**0.52**	–	**0.20**
$M_{(\Delta f<1\%)}$	–	**4**	–	**5**	–	**5**	–	**5**	–	**4**	–	**5**

Table 7. Frequency values of the vibration modes estimated from the candidate OSP configurations in the second damage scenario (DS_2). Average frequency percentage error and number of identified modes with $\Delta f<1\%$ are highlighted in bold

DS_2	OSP1		OSP2|OSP5|OSP8		OSP3		OSP4		OSP6		OSP7	
	EfI		EVP|WDPR|NODP		MSSP		ADPR		QRD		VM	
Mode	f (Hz)	$\|\Delta f\|$(%)	f (Hz)	$\|\Delta f\|$(%)	f (Hz)	$\|\Delta f\|$(%)	f (Hz)	$\|\Delta f\|$(%)	f (Hz)	$\|\Delta f\|$(%)	f (Hz)	$\|\Delta f\|$(%)
1	3.85	0.00	3.85	0.00	3.85	0.00	3.85	0.00	3.84	0.26	3.85	0.03
2	4.70	0.21	4.71	0.43	4.71	0.43	4.71	0.43	4.71	0.43	4.71	0.32
3	9.86	1.13	9.74	0.10	9.72	0.31	9.75	0.00	9.73	0.21	9.75	0.00
4	10.19	0.10	10.20	0.20	10.21	0.29	10.19	0.10	10.19	0.10	10.19	0.07
5	11.37	2.90	11.70	0.09	11.73	0.17	11.72	0.09	11.75	0.34	11.72	0.07
Avg	–	**0.87**	–	**0.16**	–	**0.24**	–	**0.12**	–	**0.27**		**0.10**
$M_{(\Delta f<1\%)}$	–	**3**	–	**5**	–	**5**	–	**5**	–	**5**		**5**

each scenario using the experimental data acquired through the full and reduced sensor configurations. As discussed in Section 3, large off-diagonal MAC terms indicate hardly distinguishable mode shapes, whereas off-diagonal MAC terms close to zero indicate orthogonality and linear independence of the identified modal vectors. The outcome is shown in Table 8. In this case, OSP2, OSP5, and OSP8 fail in the accurate identification of the mode shapes across all scenarios as the average of the off-diagonal terms of the AutoMAC matrix is the highest; hence, the identified sub-optimal set of measurement points is not adequate to ensure the extraction of linearly independent vibration modes. Similar considerations can be drawn for configurations OSP3, OSP4, and OSP7. Conversely, both heuristics that account for sensor interaction (EfI and QRD) provide better placements (OSP1 and OSP6, respectively).

Table 9 reports an overall quantitative metric comparison among the analyzed algorithms and their respective candidate sensor locations for the Z24, simultaneously considering all criteria defined in Section 4.3. As different metrics can yield distinct (sub) optimal solutions, incorporating both frequency- and mode shape-related metrics in the final assessment is crucial. Additionally, it is worth stressing again that validating the baseline sensor layout against probable DSs becomes essential to guarantee the robustness and long-term effectiveness of the monitoring system.

As previously highlighted, considering only frequency-related metrics, OSP3 is found to perform best in the RS, while OSP2/OSP5/OSP8, OSP4, and OSP7 emerge as the optimal solutions when accounting for potential damage mechanisms. On the other hand, taking into account all mode shape-related metrics, it is noted that OSP2, OSP5,

Table 8. Average of the off-diagonal terms of the AutoMAC matrices estimated for each scenario using the data acquired through the full (FSP) and reduced (OSP) configurations

	FSP	OSP1	OSP2|OSP5|OSP8	OSP3	OSP4	OSP6	OSP7
RS	0.078	0.100	0.275	0.270	0.260	0.061	0.153
DS_1	0.050	0.104	0.350	0.249	0.226	0.067	0.301
DS_2	0.053	0.138	0.341	0.264	0.247	0.161	0.307
Avg	**0.060**	**0.114**	**0.322**	**0.261**	**0.244**	**0.096**	**0.254**

Table 9. Modal-based multi-criteria optimization: comparison of frequency- and mode shape-related metrics for each candidate configuration (the best metrics are highlighted in grey)

		FSP	OSP1	OSP2|OSP5|OSP8	OSP3	OSP4	OSP6	OSP7
No. modes ($\Delta f < 1\%$)	RS	5	4	5	5	5	4	5
	DS_1	5	4	5	5	5	4	5
	DS_2	5	3	5	5	5	5	5
	Avg	**5**	**3.67**	**5**	**5**	**5**	**4.33**	**5**
Average $\lvert\Delta f\rvert(\%)$	RS	0.00	0.41	0.30	0.23	0.29	0.99	0.29
	DS_1	0.00	0.64	0.12	0.32	0.22	0.52	0.20
	DS_2	0.00	0.87	0.16	0.24	0.12	0.27	0.10
	Avg	**0.00**	**0.64**	**0.19**	**0.26**	**0.21**	**0.59**	**0.20**
Average off-diag AutoMAC	RS	0.08	0.10	0.28	0.27	0.26	0.06	0.15
	DS_1	0.05	0.10	0.35	0.25	0.23	0.07	0.30
	DS_2	0.05	0.14	0.34	0.26	0.25	0.16	0.31
	Avg	**0.06**	**0.11**	**0.32**	**0.26**	**0.24**	**0.10**	**0.25**
(1-MAC) Full vs. OSP	RS	0.00	0.05	0.08	0.11	0.17	0.08	0.43
	DS_1	0.00	0.03	0.03	0.03	0.03	0.04	0.03
	DS_2	0.00	0.07	0.01	0.04	0.03	0.04	0.02
	Avg	**0.00**	**0.05**	**0.04**	**0.06**	**0.08**	**0.05**	**0.16**
Mode shape covariance ratio	RS	−26.22	−2.93	87.91	−9.69	4.47	−3.97	3.68
	DS_1	−6.32	−1.68	55.99	−4.88	2.19	−2.32	2.19
	DS_2	− 4.27	−0.61	19.27	−2.94	1.02	−0.87	0.80
	Avg	**−12.27**	**−1.74**	**54.39**	**−5.84**	**2.56**	**−2.39**	**2.22**

Table 10. Identification of recurrent regions for best sensor placement through a local maxima approach

Algorithm	Optimal channel locations and directions		
	Side span (Utzenstorf)	Mid span	Side span (Koppigen)
MSSP	7z	18z–26z	37z
EVP	8z	18z–25z	35z–37z
VM	7z	17z–21z–24z	37z
NODP	6z–8z–11z	19z–21z–23z–25z–33z	40z
ADPR	7z	19z–22z–24z	37z
WDPR	8z –11z	18z–21z–23z–25z	35z–39z

and OSP8 reduced configurations ensure the identification of mode shapes that closely resemble those estimated from the full configuration and feature the highest ratio of diagonal to off-diagonal covariance terms; however, they fail in the accurate identification of modes across all scenarios as the average of the off-diagonal terms of the AutoMAC matrix is the highest. This means that the identified sub-optimal set of measurement points is fairly good but not fully adequate to ensure the extraction of linearly independent vibration modes. Instead, the configurations derived from the algorithms exploiting sensor interaction, namely OSP1 and OSP6, are the only ones featuring channels also in transversal direction and that perform better in terms of mode shape identifiability across all scenarios although the strength of each mode contribution is not very high because of the non-clustered distribution of sensors in the regions of modal maxima. The remaining configurations (OSP3, OSP4, and OSP7) are excluded from the final placement selection due to their poor overall metrics.

These comparative analyses make clear the difficulties associated with selecting a univocal optimal solution. Thus, to enhance the final placement performance, recurrent regions are strategically identified through a local maxima approach (Table 10), setting the number of minimum required sensors equal to the number of target modes of the undamaged bridge in the vertical direction.

By combining standard and local maxima approaches, nodes 8, 18, 19, 25, and 37 emerge as the most recurrent non-clustered measurement points to optimize bridge modal information retrieval from sensors while minimizing SHM

Table 11. Comparison of frequency values between corresponding vibration modes estimated from the full and final configurations across all scenarios

	Mode	RS			DS1			DS2		
		f_{full} (Hz)	f_{best} (Hz)	$\|\Delta f\|$(%)	f_{full} (Hz)	f_{best} (Hz)	$\|\Delta f\|$(%)	f_{full} (Hz)	f_{best} (Hz)	$\|\Delta f\|$(%)
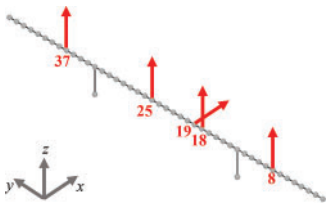	1	3.88	3.88	0.00	3.69	3.69	0.00	3.85	3.85	0.00
	2	5.02	5.02	0.00	4.92	4.92	0.00	4.69	4.66	0.64
	3	9.86	9.84	0.20	9.27	9.21	0.65	9.75	9.71	0.41
	4	10.28	10.29	0.10	9.66	9.66	0.00	10.18	10.15	0.29
	5	12.69	12.77	0.63	12.19	12.39	1.64	11.71	11.73	0.17
	Avg	–	–	**0.19**	–	–	**0.46**	–	–	**0.30**
	$M_{(\Delta f<1\%)}$	–	–	**5**	–	–	**4**	–	–	**5**

Table 12. Mode shape-related metrics for the final sensor configuration

	RS	DS1	DS2	Avg
Avg off-diag AutoMAC	0.08	0.06	0.08	0.07
(1-MAC) Full vs. OSP	0.06	0.03	0.02	0.04
Mode shape covariance ratio	−2.15	−3.31	−2.39	−2.62

equipment installation and maintenance costs. Considering these findings and expert judgment insights, the sensor placement shown in Table 11 is ultimately selected as best for the case study under consideration. As a backward validation, both frequency- and mode shape-related metrics are computed across all scenarios for the final optimal configuration. The outcome is reported in Tables 11 and 12. Since mode shapes are more effective and reliable in localizing structural damage compared to frequencies, which are easy to identify but may exhibit similar changes for different damage locations,[30] mode shape-related metrics are given greater weight than frequency-related metrics when assessing the effectiveness of the sensor placement. Accordingly, the chosen configuration results as best in terms of mode shape identifiability across all scenarios.

Conclusions

This paper explored and discussed two well-established classes of heuristic algorithms for the optimal placement of sensors in the context of multi-span bridge monitoring. Particularly, eight heuristics were investigated: (1) NODP; (2) EVP; (3) MSSP; (4) ADPR; (5) WDPR; (6) VM; (7) QRD; and (8) EfI. While the first six are individual sensor ranking algorithms, the last two rank sensors according to their interaction. In the first part of this study, the performance metrics of the aforementioned algorithms were examined through four analytical examples of beam-like systems with varying boundary conditions. Subsequently, the effectiveness of the selected OSP algorithms was evaluated through their application to a real-world bridge structure, also exploring alternative ranking solutions to refine the identification of the final best sensor placement among multiple near-optimal candidate configurations. Focusing on a data-driven approach, any computational costs and resources related to the generation and updating of complex numerical models representative of the real structure are avoided. The actual computational effort is limited to extracting modal properties from signals recorded in the ambient vibration campaign and applying the heuristic algorithms.

The main conclusions drawn from the study can be summarized as follows:

- In their basic version, heuristic algorithms for OSP tend to concentrate sensors within limited regions, and none of them provide prior information on the optimal number of sensors required. Moreover, depending on the adopted metric, sub-optimal solutions can vary significantly.
- Alternative ranking solutions that exploit the local maxima of the metric functions, rather than their maximum values, can overcome the problem of sensor clustering and provide a rapid approach to determining the optimal number of sensors required for a given set of target modes. However, this approach is more suitable for mode shapes involving displacement components in a single plane and for beam-like structures. A generalization of the method for mode shapes involving displacements along multiple directions and considering a 3D distribution of the candidate nodes is currently under development.
- Regardless of the approach, sensor distribution is always highly dependent on the number and characteristics of the chosen target modes.
- A modal-based multi-criteria optimization can be used to enhance the selection of the optimal sensor

placement among different and apparently equivalent sub-optimal candidate solutions. Multi-objective optimization that accounts for sensor installation and maintenance costs should also be considered to fully address the OSP problem.

- Since mode shapes are more effective and reliable in localizing structural damage compared to frequencies, mode shape-related metrics should be given greater weight than frequency-related metrics when assessing the effectiveness of the sensor placement.
- While the applied multi-criteria optimization framework remains valid for any type of bridge and with the addition of more DSs, the resulting optimal sensor layout is strictly case-specific and should be validated against diverse realistic failure mechanisms to guarantee the robustness and long-term effectiveness of the monitoring system. However, it is important to note that OSP is always performed prior to monitoring and before any damage occurrence. Therefore, including damage information in the optimization process is only feasible following a model-based approach, provided that DSs can be accurately simulated—which is often arguable in many practical situations.
- Fault tolerance is a critical aspect when the SHM network consists of a reduced configuration of optimal acquisition channels distributed across a large structure. A minimum number of sensors able to guarantee an "analytical redundancy" approach in the targeted regions should always be conceived, along with lightweight data duplication systems.

Acknowledegments

The authors would like to express their gratitude to the KU Leuven Structural Mechanics Section for providing the data on the Z24 bridge used in this study. This work was partly financed by FCT/MCTES through national funds (PIDDAC) under the R&D Unit Institute for Sustainability and Innovation in Structural Engineering (ISISE), under reference UIDB/04029/2020 (doi.org/10.54499/UIDB/04029/2020), and under the Associate Laboratory Advanced Production and Intelligent Systems ARISE under reference LA/P/0112/2020.

References

[1] Song Y, Jin H. A sensitivity based method for sensor placement optimization of bridges. *SPIE 6932, Sensors and Smart Structures Technologies for Civil, Mechanical, and Aerospace Systems*; 2008:69323W. doi:10.1117/12.776049

[2] Ostachowicz W, Soman R, Malinowski P. Optimization of sensor placement for structural health monitoring: a review. *Struct Health Monitor*. 2019;18(3):963–988. doi:10.1177/1475921719825601.

[3] Civera M, Pecorelli ML, Ceravolo R, Surace C, Zanotti Fragonara L. A multi-objective genetic algorithm strategy for robust optimal sensor placement. *Comput-Aided Civil Infrastruct Eng*. 2021;36(9):1185–1202. doi:10.1111/mice.12646.

[4] Masciotta MG, Barontini A, Brando G, Lourenço PB. Optimization of sensor configurations for cost-efficient monitoring of infrastructure systems. In: Limongelli MP, Giordano PF, Quqa S, Gentile C, Cigada A, eds. *Experimental Vibration Analysis for Civil Engineering Structures. EVACES 2023. Lecture Notes in Civil Engineering*. vol. 432. Cham: Springer; 2023. doi:10.1007/978-3-031-39109-5_36.

[5] Masciotta MG, Barontini A, Pellegrini D, Brando G, Lourenço PB. Optimal sensor placement for bridge structural health monitoring: Integration of physics-based models with data-driven approaches. *Procedia Struct Integr*. 2024;62:932–939. doi:10.1016/j.prostr.2024.09.125.

[6] Glassburn RS, Smith SW. Evaluation of sensor placement algorithms for on-orbit identification of space platforms. *NASA Conference Publication*; Baltimore, MD (United States); 1994:333.

[7] Padula SL, Palumbo DL, Kincaid RK. Optimal sensor/actuator locations for active structural acoustic control. *AIAA*; 1998. Paper 98-1865. doi:10.2514/6.1998-1865

[8] Naimimohasses DM, Barnett DM, Green DA, Smith PR. Sensor optimization using neural network sensitivity measures. *Meas Sci Technol*. 1995;6(9):1291–1300. doi:10.1088/0957-0233/6/9/008.

[9] Oh DY, No HC. Determination of the minimal number and optimal sensor location in a nuclear system with fixed incore detectors. *Nuclear Eng Design*. 1994;152(1–3):197–212. doi:10.1016/0029-5493(94)90085-X.

[10] Meo M, Zumpano G. On the optimal sensor placement techniques for a bridge structure. *Eng Struct*. 2005;27(10):1488–1497. doi:10.1016/j.engstruct.2005.03.015.

[11] Chow HM, Lam HF, Yin T, Au SK. Optimal sensor configuration of a typical transmission tower for the purpose of structural model updating. *Struct Control Health Monitor*. 2011;18(3):305–320. doi:10.1002/stc.372.

[12] Pachón P, Castro R, García-Macías E, Compan V, Puertas EE. Torroja's bridge: Tailored experimental setup for SHM of a historical bridge with a reduced number of sensors. *Eng Struct*. 2018;162(3):11–21. doi:10.1016/j.engstruct.2018.02.035.

[13] Imposa G, Barontini A, Lourenco PB, Russo S. A strategy of optimal sensor placement for dynamic identification in cultural heritage. *RILEM Bookseries*. 2024;47:309–321. doi:10.1007/978-3-031-39603-8_26.

[14] Chaves E, Barontini A, Mendes N, Compán V, Lourenço PB. Methodologies and challenges for optimal sensor placement in historical masonry buildings. *Sensors*. 2023;23(23):9304. doi:10.3390/s23239304.

[15] Lenticchia E, Ceravolo R, Antonaci P. Sensor placement strategies for the seismic monitoring of complex vaulted structures of the modern architectural heritage. *Shock Vibr*. 2018;1–14. doi:10.1155/2018/3739690.

[16] Nicoletti V, Quarchioni S, Amico L, Gara F. Assessment of different optimal sensor placement methods for dynamic monitoring of civil structures and infrastructures. *Struct Infrastruct Eng*. 2024;2768(1):1–16. doi:10.1080/15732479.2024.2383299.

[17] Tan Y, Zhang L. Computational methodologies for optimal sensor placement in struc-tural health monitoring: a review. *Struct Health Monitor*. 2020;19(4):1287–1308. doi:10.1177/1475921719877579.

[18] Vinod Chandra SS, Anand HS. Nature inspired meta heuristic algorithms for optimization problems. *Computing*. 2022;104(2):251–269. doi:10.1007/s00607-021-00955-5.

[19] Barontini A, Masciotta MG, Ramos LF, Amado-Mendes P, Lourenço PB. An overview on nature-inspired optimization algorithms for Structural Health Monitoring of historical buildings. *Procedia Eng*. 2017;199(5):3320–3325. doi:10.1016/j.proeng.2017.09.439.
[20] Imamovic N. *Model Validation of Large Finite Element Model Using Test Data*. PhD thesis. Imperial College, London, UK; 1998.
[21] DeClerck JP, Avitabile P. Development of several new tools for modal pre-test evaluation. *Proceedings of the 14th International Modal Analysis Conference (IMAC)*; Dearborn, Michigan; 1996:2768, 1272.
[22] Doebling SW. *Measurement of Structural Flexibility Matrices for Experiments With Incomplete Reciprocity*. PhD dissertation. Colorado University, USA; 1995.
[23] Chung YT, Moore D. On-Orbit sensor placement and system identification of space station with limited instrumentations. *Proceedings of the 11th International Modal Analysis Conference (IMAC)*; Kissimmee, Florida; 1993:41–46.
[24] Schedlinski C, Link M. An approach to optimal pick-up and exciter placement. *Proceedings of SPIE—The International Society for Optical Engineering*; Denver, Colorado; 1996: 376–382.
[25] Kammer DC. Sensor placement for on-orbit modal identification and correlation of large space structures. *J Guid, Control, Dyn*. 1991;14(2):251–259. doi:10.2514/3.20635.
[26] De Roeck G. The state-of-the-art of damage detection by vibration monitoring: the SIMCES experience. *J Struct Control*. 2003;10(2):127–143. doi:10.1002/stc.20.
[27] Peeters B, De Roeck G. One-year monitoring of the Z24-Bridge: environmental effects versus damage events. *Earthq Eng Struct Dyn*. 2001;30(2):149–171. doi:10.1002/1096-9845(200102)30:2<149::AID-EQE1>3.0.CO;2-Z.
[28] Maeck J, De Roeck G. Description of Z24 benchmark. *Mech Syst Signal Process*. 2003;17(1):127–131. doi:10.1006/mssp.2002.1548.
[29] Teughels A, De Roeck G. Structural damage identification of the highway bridge Z24 by FE model updating. *J Sound Vibr*. 2004;278(3):589–610. doi:10.1016/j.jsv.2003.10.041.
[30] Masciotta MG, Pellegrini D. Tracking the variation of complex mode shapes for damage quantification and localization in structural systems. *Mech Syst Signal Process*. 2022;169(5):108731. doi:10.1016/j.ymssp.2021.108731.